

## RESEARCH

# SPIKE: Secure and Private Investigation of the Kidney Exchange problem

Timm Birka<sup>1†</sup>, Kay Hamacher<sup>2</sup>, Tobias Kussel<sup>2</sup>, Helen Möllering<sup>1\*</sup> and Thomas Schneider<sup>1</sup>

## Abstract

**Background:** The kidney exchange problem (KEP) addresses the matching of patients in need for a replacement organ with compatible living donors. Ideally many medical institutions should participate in a matching program to increase the chance for successful matches. However, to fulfill legal requirements current systems use complicated policy-based data protection mechanisms that effectively exclude smaller medical facilities to participate. Employing secure multi-party computation (MPC) techniques provides a technical way to satisfy data protection requirements for highly sensitive personal health information while simultaneously reducing the regulatory burdens.

**Results:** We have designed, implemented, and benchmarked SPIKE, a secure MPC-based privacy-preserving KEP which computes a solution by finding matching donor–recipient pairs in a graph structure. SPIKE matches 40 pairs in cycles of length 2 in less than 4 minutes and outperforms the previous state-of-the-art protocol by a factor of 400× in runtime while providing medically more robust solutions.

**Conclusions:** We show how to solve the KEP in a robust and privacy-preserving manner achieving practical performance. The usage of MPC techniques fulfills many data protection requirements on a technical level, allowing smaller health care providers to directly participate in a kidney exchange with reduced legal processes.

**Keywords:** Kidney-Exchange; Privacy; Secure Multi-Party Computation (MPC)

## Introduction

Around 7% of U.S. adults are affected by chronic kidney disease [1]. With the increasing age of the population in most countries, end-stage renal disease constitutes a rapidly increasing challenge for health care systems [2]. Humans are able to live a normal life with at least one functioning kidney [3]. However, when both kidneys of a person are malfunctioning, this person requires kidney replacement therapy to survive, i.e., either dialysis or the donation of a functioning kidney.

Transplantations of deceased donor organs unfortunately imply long waiting times as transplant waiting lists grow, given that the number of donations significantly exceed supply [4]. The other option is to find a living person that is willing to donate one of their kidneys. In general, living donor donations result in shorter waiting times and tend to have better long term outcomes compared to deceased donor donations [5]. Unfortunately, finding a willing, living donor does not guarantee (medical) compatibility with the

recipient. Hence, the living donor exchange system was introduced in 1991 [6], which allows recipients with incompatible living donors, in the following referenced as *pairs*, to exchange their donors such that ideally each recipient can receive a compatible kidney donation.

In this work, we consider a scenario in which several pairs exchange their donors in a cyclic fashion, so that each donating pair receives a compatible kidney. These cycles are called *exchange cycles* [7].

As a first step for finding possible exchange cycles, we have to evaluate the donors' and recipients' medical data to determine compatibility between pairs. Afterwards, we have to identify possible exchange cycles. This problem is known as the kidney exchange problem (KEP) [7] and can be described as finding cycles in a directed graph where each vertex represents a pair and a directed edge describes the compatibility between two pairs. A schematic view of the protocol can be seen in Figure 1.

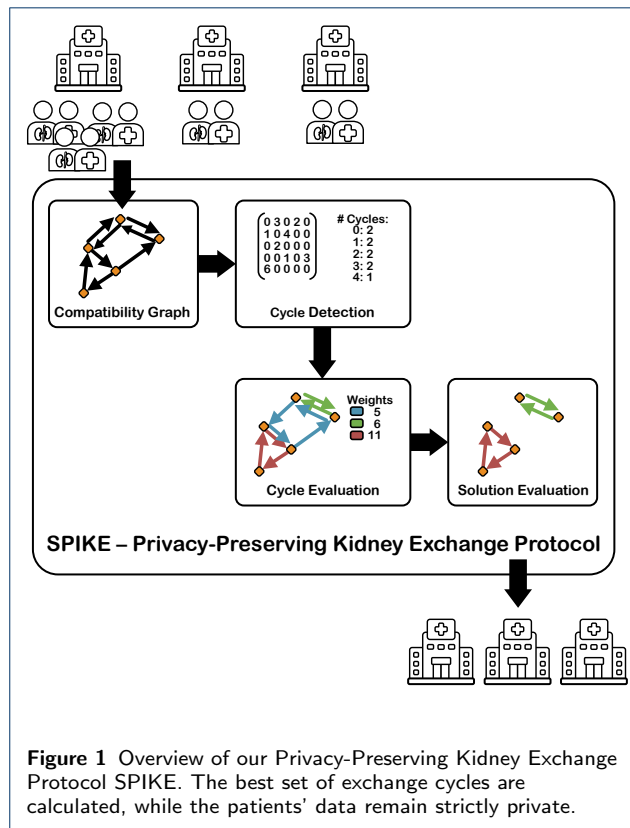
The process requires the analysis of highly sensitive medical health data, which makes it crucial that no information is leaked accidentally or to unauthorized personnel. Thus, KEP requires the implementation of

\*Correspondence: [moellering@crypto.cs.tu-darmstadt.de](mailto:moellering@crypto.cs.tu-darmstadt.de)

<sup>1</sup>ENCRYPTO, Technical University of Darmstadt, Darmstadt, Germany

Full list of author information is available at the end of the article

<sup>†</sup>Lead Author



strong privacy-preserving solutions where the plaintext health information remains locally at each medical institution and the analysis is only run on “encrypted” data which is leaking nothing beyond the output: an exchange cycle with high transplantation success likelihood.<sup>[1]</sup> Note that such a distributed solution also enhances security against data breaches as having to attack multiple parties is significantly harder than a single target. Similarly, it also simplifies the compliance with regulatory requirements potentially complicating or even prohibiting data sharing among facilities.

### Contributions and Outline

In this work, we provide the following contributions:

- **Efficient Privacy-Preserving Kidney Exchange protocol:** We design and implement SPIKE, an efficient, distributed, privacy-preserving protocol for solving the kidney exchange problem in the semi-honest security model. In contrast to the current state-of-the-art [8, 9], SPIKE improves the medical compatibility matching by considering additional factors, namely, age, sex, human leukocyte antigens, and weight, that significantly affect compatibility between potential

donors and recipients and is, thus, more robust than previous solutions by reducing the risk of failing procedures.

- **Comprehensive Empirical Evaluation:** We implement and extensively benchmark SPIKE and show that it has practical runtimes and communication costs. We achieve about  $30\,000\times$  speedup over [8] and  $400\times$  over [9] thanks to our carefully optimized hybrid secure multi-party computation (MPC) protocols. Further, we provide additional (micro-) benchmarks and network settings to further demonstrate scalability and practicality of SPIKE.
- **Open-source Implementation:** SPIKE is available under the GNU LGPL v3 license<sup>[2]</sup> here: <https://encrypto.de/code/PPKE>.

### Related Work

In this section, we summarize the related work on the Kidney Exchange Problem (KEP) with and without considering data privacy.

#### Robust KEP

One major issue in kidney exchange programs is the potential cancellation of transplantations *after* having already determined exchange cycles of compatible donors and recipients. Reasons for such cancellations are manifold, e.g., a donor withdraws his consent as his non-compatible relative has already received a kidney via the waiting list from a deceased donor in the meantime [10]. These issues call for *robust* solutions to the KEP, i.e., flexibility for recipient/donor dropouts and including as much as possible medical factors that can be algorithmically evaluated.

Carvalho et al. [11] propose three policies that are able to cope with dropouts within an kidney exchange cycle. One takes the costs (or missed gains) of planned transplants that do not proceed into account to find a solution with high probability of being successfully executed. The other two policies investigate strategies for recovering exchange cycles after dropouts. The plaintext algorithms in [11] are computationally expensive and, thus, cannot be trivially realized as secure computation protocols.

Ashby et al. [12] introduce a calculator for determining compatibility in kidney exchange which they use to evaluate the importance of various medical factors such as age, sex, obesity, weight, height, human leukocyte antigen (HLA) mismatches and ABO blood groups (see Section “Medical Background”). In our work, we increase the robustness of our privacy-preserving kidney exchange protocol by including the

<sup>[1]</sup>This cycle still requires a final check by medical experts.

<sup>[2]</sup><https://www.gnu.org/licenses/lgpl-3.0>

additional important biomedical factors from [12]. Furthermore, we recommend to use cycle sizes of two or three to reduce the impact of withdrawals [10]. The size is also beneficial for practical considerations with respect to medical staff and other resources needed for transplantations as all operations of one exchange cycle should ideally be executed simultaneously. This recommendation reflects current best practices [13].

#### *Privacy-preserving KEP*

Just two works, both by Breuer et al. [8, 9], investigate how to solve the kidney exchange problem in a decentralized privacy-preserving manner. Both consider the semi-honest security model.

*Privacy-preserving KEP with HE.* The first protocol [8] uses homomorphic encryption (concretely, a threshold variant of the Paillier cryptosystem [14]). It instantiates a computing party for each pair of a non-compatible donor and recipient at the providing hospital, thus, effectively creating a multi-party computation (MPC) protocol.

The protocol first pre-computes a set of all possible exchange constellations independent of any input data. Cycles of all lengths up to 3 are computed (but an arbitrary value could be chosen). Next, the pairs jointly compute an adjacency matrix with the pairwise compatibility based on HLA crossmatching and ABO blood groups. Combining the results with the exchange constellations, the graph with the maximal size is delivered as the output. The protocol's runtime scales exponentially with the number of pairs: starting with a runtime of 14 seconds for two pairs it increases to 13 hours for nine pairs. Unfortunately, such runtimes are prohibitive for practical deployment.

*Privacy-preserving KEP with Shamir's Secret Sharing.* In a concurrent work to ours, Breuer et al. [9] introduced a privacy-preserving KEP protocol for crossover kidney exchanges with polynomial computation complexity. "Crossover" hereby means that the kidney exchange is done among two pairs, i.e., the exchange cycle size is limited to two in contrast to [8]. This limitation, however, enables a significant efficiency improvement for matchings with more than 13 pairs. For example, with 15 pairs it reduces the runtime of the old protocol [8] from 8.5 hours to 30 minutes. Additionally, the new protocol enables a dynamic setting where donor-recipient pairs can be added/removed from the exchange graph at any point in time. On the technical side, the authors replace HE and fully rely on a MPC-technique called Shamir's Secret Sharing (SSS) [15] implemented with the MP-SPDZ framework [16]. Beyond the dynamic setting and the change to MPC, the new protocol employs the graph matching algorithm by Pape and Conradt [17]

for better efficiency in the matching between compatible donors and recipients.

Our privacy-preserving KEP protocol SPIKE offers practical runtimes for real-world deployment. Our runtimes significantly outperform the measured runtimes of previous works [8, 9], e.g., by a factor of hundreds/thousands for 9 recipient-donor pairs with a cycle length of 2. This is due to an efficient symbiosis of three MPC techniques and protocol optimizations that we will detail in the next section. Furthermore, we improve the robustness of SPIKE by including four additional biological factors notably impacting the transplantation success rate [12]. Thus, our protocol focuses on high medical quality rather than pure size while also significantly improving efficiency.

## Background

In this work, we present a privacy-preserving solution to the *kidney exchange problem* (KEP). We interpret the KEP as an optimization problem, specifically finding cycles with a maximal coverage of nodes on a compatibility graph and a maximal aggregated edge weight. The graph is constructed according to medical compatibility factors. This section gives the required background information to understand the underlying aspects of biomedicine, graph theory, as well as the used privacy-preservation techniques of secure multi-party computation (MPC).

### Medical Background

In the following, we introduce the medical background, i.e., biological factors used in our protocol that cause general immunological incompatibility or influence success likelihood for a kidney transplantation.

#### *General immunological compatibility*

While many medical factors are involved in the definite assessment of donor-recipient compatibility, some can be algorithmically determined. For example, one key factor in avoiding allograft rejection—immunological compatibility—can be evaluated following evidence-based guidelines. Our kidney exchange protocol uses a specific form of immunological compatibility, the HLA crossmatch, as a transplant prohibiting factor.

*Human Leukocyte Antigens crossmatch.* The human immune system is responsible for the protection of the organism against potentially harmful invaders (called *pathogens*). Antigens are molecular structures often found on the surface of pathogens, but also naturally occurring in the body. *Antibodies* can attach to those structures, preventing the pathogens from docking, thus inhibiting their harmful effect. One important group of endogenous antigens which occur in varying numbers in every human, forming the immunological

“fingerprint” the immune system recognizes as normal, are the *human leukocyte antigens*. Out of the three classes of HLA [18], only classes I and II are of interest in this work.

With a *HLA crossmatch* general compatibility between recipient and donor can be determined: The human leukocyte *antigens* of a donor are matched against existing human leukocyte *antibodies* of a possible recipient [19]. HLA crossmatch positive kidney transplants carry a significantly higher risk of antibody-mediated rejection or allograft rejection due to already existing antibodies [20, 21]. Modern immunosuppressants might make such a procedure possible [22], but those cases require specialized, in-depth medical assessment and are out of scope of a general, algorithmic evaluation.

Following Eurotransplant’s guidelines [19], we consider HLA groups, which are also most frequently screened in preparation for kidney replacement therapy [23]: the HLA encoded at HLA-A, -B, and -DR loci. Additionally, we consider the HLA-DQ coded antigens, which are related to some cases of antibody-mediated rejection [24]. The full list of HLA considered in SPIKE can be seen in Table 1.

**Table 1** HLA split antigens assessed for biomedical donor – recipient compatibility testing in SPIKE.

Class I		Class II		
HLA-A	HLA-B	HLA-DR	HLA-DQ	
A23	B38	B60	DR11	DQ5
A24	B39	B61	DR12	DQ6
A25	B44	B62	DR13	DQ7
A26	B45	B63	DR14	DQ8
A29	B49	B64	DR15	DQ9
A31	B50	B65	DR16	
A32	B51	B71	DR17	
A33	B52	B72	DR18	
A34	B54	B75		
A66	B55	B76		
A68	B56	B77		
A69	B57			
A74	B58			

#### Match quality estimation

Additionally to the previously introduced procedure that prevents immunological incompatibility, we strive to find the medically best/most robust solution to the kidney exchange problem – that includes maximal survival probability. For that, we calculate a match quality index, based on the following additional medical factors:

(i) *HLA match*.

Additionally to the HLA crossmatch, HLAs influence the probability of a successful transplantation. Concretely, it increases if the donor has

a subset or the same HLA as the recipient. The number of “mismatches” is associated with increased allograft rejection rates, as the probability that a recipient develops antibodies to those mismatched antigens increases [25]. HLA mismatches do not constitute exclusion criteria, as immunosuppressants can reduce the rejection probability. The use of immunosuppressants, however, is itself linked to higher rejection rates [25–27]. Special importance comes to the HLA-DQ group, as mismatches of it are strongly linked to antibody-mediated rejections [24].

Each person can inherit up to two types of HLA per group. Hence, at most two mismatches can occur per group [28]. The impact of HLA mismatches can be categorized in four bins: having no mismatch, a very rare case and mostly occurring in twin donor-recipient pairs, having 1 to 2 mismatches, having 3 to 4 mismatches, and, worst of all, having more than 5 mismatches [25]. The last group shows a more than 6% cumulative risk for death with a functioning graft during the first year. We weight HLA mismatches according to those four categories.

- (ii) *ABO blood type*. The ABO blood type system is based on the presence or absence of two types of antigens on the surface of the red blood cells [29]. The absence of both type A and type B antigens mark blood type O, the presence of both mark blood type AB, and the presence of only one mark blood type A and B, respectively. Receiving blood with an incompatible blood type leads to blood clumping due to an immune reaction and a possibly failed procedure. Compatible pairings are given in Table 2.

By pre-processing the donor organ, grafts from ABO incompatible donors are possible [30], although linked to severe adversary reactions during the first year post transplantation. These reactions include a higher risk of allograft loss, severe viral infections, antibody-mediated rejections, and postoperative bleeding. After this first year, however, the long-term survival rate is comparable to ABO compatible transplants [30].

**Table 2** ABO compatibility [29]

Blood Group	Can Receive From	Can Donate To
O	O	O, A, B, AB
A	O, A	A, AB
B	O, B	B, AB
AB	O, A, B, AB	AB

- (iii) *Age*. According to Waiser et al. [31], also age disparity influences allograft survival post transplant. The authors examined the role of age of

the donor and recipient using two categories: *junior* participants aged below 55 years and *seniors* participants older than 55 years. The results show that intra-categorical transplants show the best outcomes, followed by pairings of junior donors and senior recipients. The worst outcomes were observed for pairings with senior donors and junior recipients.

- (iv) *Sex*. As shown by Zhou et al. [32], the combination of donor-recipient sexes impact the transplant success probability. The worst allograft survival rates were observed in male recipients for female donor organs, while same-sex pairs performed slightly better than female recipients for male donor organs.
- (v) *Weight*. Recipients who received a kidney from a donor who weighs less have higher chances of allograft loss than other recipients [33]. El-Agroudy et al. [34] reason that the allograft loss for recipients with kidneys from lighter donors might be caused by the kidney being unable to support the body functions of a heavier recipient.

### Graph Theory

We represent the structure of the kidney exchange problem (KEP) as a (bipartite) graph problem. A graph  $\mathcal{G}$  consists of a set of vertices  $\mathcal{V}$  and an edge set  $\mathcal{E}$  connecting the vertices. Technically, we deal with a *bipartite* graph, i.e., consisting of two different sets of vertices (donors and recipients), but as those register pairwise for the kidney exchange, we can “collapse” each donor-recipient pair into one vertex in  $\mathcal{V}$ . If two vertices  $v, u \in \mathcal{V}$  are connected by an edge, then  $(v, u) \in \mathcal{E}$ . We consider a directed graph with directed edges from  $v$  to  $u$ . Furthermore, we use *weighted* edges by associating a scalar weight to each edge, according to its “importance” in the network. The weights represent the degree of medical compatibility. We only allow positive edge weights.

Our goal is to find all cycles within the graph. A cycle  $c$  is a list of vertices  $\{v_1, v_2, \dots, v_m\}$  where an edge exists from vertex  $v_i$  to  $v_{i+1}$  for  $i \in \{1, \dots, m-1\}$  and, to close the “loop”, from vertex  $v_m$  back to vertex  $v_1$ . In a vertex disjoint cycle, each vertex appears at most once within the cycle. We define the length of a cycle as the number of edges that are used to form that cycle.

One representation of a (weighted) graph structure is the *adjacency matrix*, a square matrix  $A$  with one row/column for each vertex. If an edge exists between vertices  $i$  and  $j$ , then, the entry  $a_{ij} = w$ , with  $w > 0$  being the edge weight and  $a_{ij} = 0$  otherwise. This work uses the fact that by raising the adjacency matrix to the  $\ell$ th power, one can quickly compute the number of paths between two vertices with a given length  $\ell$ .

That means, that vertices  $i$  and  $j$  are connected by  $(A^\ell)_{ij}$  paths of length  $\ell$ . The diagonal elements give the number of cycles of length  $\ell$  by finding paths starting and ending on the same vertex.

### Secure Computation

Secure computation techniques enable multiple parties to securely evaluate an arbitrary function on their private inputs. Ideally nothing is leaked beyond what can be inferred from the output. A secure computation protocol must be able to realize this functionality without relying on a trusted party. To verify its security, it is typically compared to the so-called *ideal functionality* which is a trusted third party that runs the computation on behalf of the data owners.

Privacy research has mainly worked on two paradigms for secure computation: Homomorphic Encryption (HE) and Secure Multi-Party Computation (MPC). HE schemes are special public-key encryption schemes that allow to realize (some limited) mathematical operations under encryption. However, they tend to be computing intensive making them (yet) often unsuitable for real-world applications. In contrast, MPC techniques are typically more efficient with respect to computation as they are mainly based on efficient symmetric encryption. Additionally, MPC protocols can compute arbitrary functions. They are typically split into a setup and an online phase where the setup phase is independent of the input data and, thus, can be pre-computed. This separation enables to significantly speed up the time-critical online phase as pre-computation can be done in idle times when input data is not yet available. However, MPC involves two or more parties who jointly evaluate the desired function in a secure manner, hence, it requires communication among the parties. Both paradigms have already been used in the context of privacy-preserving genome-wide association studies [35–37] as well as other applications in the health care area [38–41].

To have provably secure privacy guarantees while achieving practical efficiency, SPIKE efficiently combines multiple MPC techniques which we introduce in the following.

### Secure Multi-Party Computation (MPC)

Introduced by Andrew Yao’s seminal work “How to Generate and Exchange Secrets” [42] in 1986, secure Multi-Party Computation (MPC) was considered a theoretical field first. MPC are cryptographic protocols that can securely compute an arbitrary function among two or more parties on their private inputs. Enabled by the rapid development of computer hardware and the development of the first MPC compiler “Fairplay” [43], first practical uses were demonstrated around the year 2004. Since then, MPC is a

**Table 3** Garbled AND Gate

Input $w_0$	Input $w_1$	Output $w_2$	Garbled Value
$k_0^{w_0}$	$k_0^{w_1}$	$k_0^{w_2}$	$Enc_{k_0^{w_0}, k_0^{w_1}}(k_0^{w_2})$
$k_0^{w_0}$	$k_1^{w_1}$	$k_0^{w_2}$	$Enc_{k_0^{w_0}, k_1^{w_1}}(k_0^{w_2})$
$k_1^{w_0}$	$k_0^{w_1}$	$k_0^{w_2}$	$Enc_{k_1^{w_0}, k_0^{w_1}}(k_0^{w_2})$
$k_1^{w_0}$	$k_1^{w_1}$	$k_1^{w_2}$	$Enc_{k_1^{w_0}, k_1^{w_1}}(k_1^{w_2})$

flourishing research field and due to novel protocols and optimizations, such as “Free XOR” [44] or “Half-gates” [45], practical applications in many fields were shown [38, 46, 47].

In this work, we rely on three well established secure *two-party* computation techniques, i.e., the secure computation protocols are run among exactly two parties: Arithmetic Secret Sharing ( $\mathcal{A}$ ), Boolean Sharing ( $\mathcal{B}$ ), both based on [48], and Yao’s Garbled Circuits ( $\mathcal{Y}$ ), originally introduced in [42]. Each technique differs in how it creates (*shares*) and reconstructs secrets, but also how (efficiently) certain types of operations can be realized.

*Notation.* In the following,  $\langle x \rangle_i^s$  denotes a secret share of  $x$  shared using MPC technique  $s \in \{A, B, Y\}$  and held by party  $P_i$ , where  $i \in \{0, 1\}$ .

*Yao’s Garbled Circuits ( $\mathcal{Y}$ ).* Yao’s Garbled Circuits enable two parties, called the *garbler* and the *evaluator*, to securely evaluate a function  $f$  represented as *Boolean circuit*, i.e., a directed acyclic graph where the nodes are logic gates and the edges (called *wires*) are the Boolean in- and outputs. For functional completeness AND and XOR gates are sufficient. The garbler generates random keys for each possible state of each wire  $k_0^w, k_1^w \in \{0, 1\}^\kappa$ , where  $\kappa$  is the symmetric security parameter (set to  $\kappa = 128$  in our implementation) and  $w$  is the respective wire. For all input combinations of each gate in the circuit, it uses the input keys to encrypt the corresponding output key (cf. Table 3). The order of the four ciphertexts is then permuted randomly and the *garbled circuit* is sent to the evaluator together with the keys associated to the garbler’s input. As those keys look random, the evaluator cannot extract any information about the input of the garbler. Next, the evaluator engages in an oblivious transfer [49, 50] to receive the keys for his input without revealing it to the garbler. Equipped with all keys, it evaluates the garbled circuit to receive the circuit’s output keys which the parties jointly decode. Thanks to several optimizations, e.g., [44, 45, 51],  $\mathcal{Y}$  requires no communication for the evaluation of an XOR gate and only  $1.5\kappa$  bits of communication for AND gates.  $\mathcal{Y}$  needs a constant number of communication rounds independent of the circuit depth.

*Boolean and Arithmetic Secret Sharing ( $\mathcal{B}/\mathcal{A}$ ).* In Additive Arithmetic Secret Sharing ( $\mathcal{A}$ ) operations on  $\ell$ -

bit inputs are done in an algebraic ring  $\mathbb{Z}_{2^\ell}$ , where  $\ell$  is the bit length. Although the technique can also be used among an arbitrary number of parties [52], we focus here on the two party setting as introduced by Goldreich et al. [48].

To share a secret value  $x$ , party  $P_i$ ,  $i \in \{0, 1\}$ , generates a random value  $r \in_R \mathbb{Z}_p$  and sets its arithmetic share to  $\langle x \rangle_i^A = r$ . Then,  $P_i$  also determines party  $P_{1-i}$ ’s share  $\langle x \rangle_{1-i}^A = x - r \bmod 2^\ell$  and sends it to  $P_{1-i}$ . To reconstruct the secret, one needs to know *both* shares and compute  $x = \langle x \rangle_0^A + \langle x \rangle_1^A \bmod 2^\ell$ . Boolean Secret Sharing ( $\mathcal{B}$ ) describes the special case where  $\ell = 1$ , viz.  $\mathbb{Z}_2 = \{0, 1\}$ .

Note that a share  $\langle x \rangle_i^A$  (resp.  $\langle x \rangle_i^B$ ) is random and does not leak anything about the secret  $x$ . Secure addition (respectively, XORing in  $\mathcal{B}$ ) can be executed locally, that is without communication between the parties. Secure multiplication (respectively, AND in  $\mathcal{B}$ ) is done in an interactive protocol among the two parties using so-called multiplication triples [53–55]. Using only addition and multiplication (similarly, AND and XOR) arbitrary functions can be calculated.

*ABY Framework.* All three MPC techniques are implemented in the state-of-the-art secure two-party computation framework ABY [54] which we use in our experiments. Additionally, ABY also contains efficient conversions between them and supports Single Instruction Multiple Data (SIMD) operations to parallelize identical operations on different data while reducing memory usage and runtime. Arithmetic Secret Sharing in ABY is performed on the ring  $\mathbb{Z}_{2^\ell}$ , that is with  $2^\ell$  elements where  $\ell$  is the bitlength of the data type (most often  $\ell = 32$  bit). A recent work by Patra et al. [46] improves [54] by making the online communication of scalar multiplication independent of the vector dimensions and reducing online communication for AND gates with two inputs in  $\mathcal{B}$  by a factor of 2. Unfortunately, these protocols have been implemented only very recently in MOTION2NX [56] which is why we use [54] in our implementation.

### Security Model

In our work, we consider the *semi-honest* security model where all involved parties are assumed to be honestly following the protocol while trying to learn as much information as possible. By “honestly following the protocol” we, thereby, mean that they adhere to the specifications of the protocol, e.g., they do not manipulate local calculations or provide inconsistent data. Additionally, the parties are assumed to not collude. This security model provides protection against curious personnel or accidental data leakage. Although weaker than the malicious security model where the parties might arbitrarily deviate from the

protocol, the semi-honest security model is sufficient for our use case, as hospitals are generally trusted but legally not allowed to simply share the data among each other. Furthermore, the semi-honest security model enables significantly more efficient computation than the malicious model and, hence, provides a good efficiency-privacy trade-off. Previous works on privacy-preserving KEP [8, 9] are also in the semi-honest security model.

### Outsourcing Data-Model

Although we use 2-party MPC to perform the computation, any number of parties can provide input data. This *outsourcing* [57] works by all data owners sharing their data and sending one share to each of the two non-colluding computation servers. Those servers, then, perform the actual secure computation on behalf of the data owners while not being able to learn anything about the private input data. This scenario has three main benefits:

- The communication of  $N$ -party MPC scales at least linearly, if not quadratic in the number of participating parties [58]. By outsourcing the  $N$ -party computation to  $M$  parties, here  $M = 2$ , the communication is improved by around  $\mathcal{O}(\frac{N}{M})$ .
- As the input owners do not participate in the computation itself, the outsourced protocol provides security against malicious data owners [57]. At most they can corrupt the correctness of the calculation, but not the privacy.
- The location of the computation servers can be chosen pragmatically, e.g., the two locations with the highest bandwidth or lowest latency network connection. Of course, the non-collusion assumption must be considered.

## Methods

In this section, we first define the privacy-preserving Kidney Exchange problem (KEP) and its requirements. Then, we present our solution, which we name SPIKE, consisting of tailored modular secure MPC protocols and include a complexity analysis.

### Problem Statement

Figure 2 shows the ideal functionality for solving the privacy-preserving KEP in a provably secure way. Assuming the (not realistic) availability of a trusted third party (TTP), hospitals send the data of recipients and donors to the TTP which calculates cycles of pairs of recipients and donors with the highest probability to be compatible. Then, the TTP returns for each recipient the information about his/her donor to the respective hospital. Note that a final evaluation must still be done by medical experts. A privacy-preserving KEP

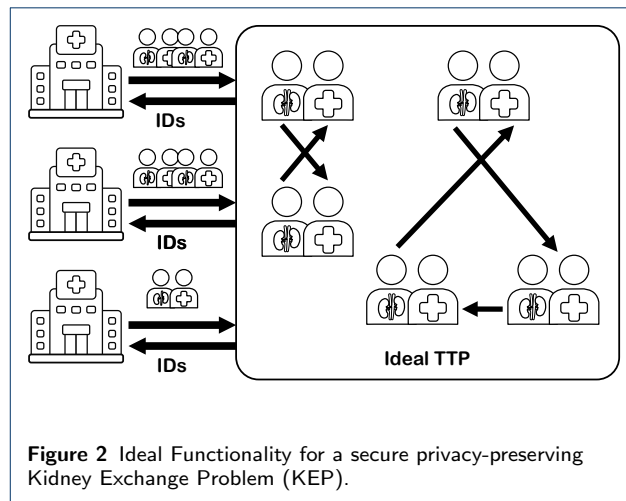


**Figure 2** Ideal Functionality for a secure privacy-preserving Kidney Exchange Problem (KEP).

is meant for automatizing and, thus, accelerating, the process of the creation of the kidney exchange cycles.

**Requirements:** We define the following requirements for a secure privacy-preserving KEP protocol:

- **Privacy.** The privacy-preserving KEP protocol must realize the same functionality as described in the ideal functionality while removing the problematic assumption of a TTP, i.e., it must leak nothing beyond what can be inferred from the output.
- **Efficiency.** The privacy-preserving KEP protocol must be efficient in terms of communication and computation such that it can be run in reasonable time on standard server hardware.
- **Decentralization.** The privacy-preserving KEP protocol must be decentralized, i.e., the highly sensitive medical information of donors and patients must remain locally at the respective medical institution (inherently being compliant with the data minimisation principle).
- **Adaptability for Medical Experts.** The privacy-preserving KEP protocol must be flexibly adaptable for medical experts with respect to the selection of biological factors for the algorithmic evaluation of compatibility. They must be able to adjust the weighting between the included factors and cycle lengths according to state-of-the-art medical advancements. The protocol must be easily extendable to new factors and additional HLA groups.

**SPIKE:** A MPC-based privacy-preserving KEP protocol  
 In this section, we provide the building blocks for our Secure and Private Investigation of the Kidney Exchange problem: SPIKE. It fulfills above requirements (see also the overview of the phases in Figure 1).

First, we explain the matching phase, which analyzes the compatibility between donors and recipients using six biological factors presented in the Background section. Then, we continue with the determination of the number of potential exchange cycles given a cycle length. The third phase computes the probability of a successful transplantation based on the matching results for all potential exchange cycles. In the final phase, we output a robust set of *disjoint* exchange cycles, i.e., with a high probability for compatibility. By design, SPIKE enables usage in a dynamic setting similar to the protocol in [9].

*Notation.* We use Boolean operators to concisely present our MPC protocols:  $\wedge$  is AND,  $\vee$  is OR,  $\neg$  is Not, and  $\oplus$  is XOR. 0/1 are False/True.  $|x|$  indicates the length of a vector  $x$ , i.e., the number of elements. Non trivial variable names in protocols are written in sans serif, function names (and calls) monospaced. Branching, implemented with MUX (multiplexer) Gates, is displayed using ternary notation: condition ? true statement : false statement.

### Compatibility Matching

The first phase of SPIKE is called *compatibility matching*. In this phase, we compare the pair-wise general compatibility and match quality of all donors and recipients with respect to human leukocyte antibodies and antigens, ABO blood group compatibility, age, sex, and weight. The output of this phase is a weighted compatibility graph where the edge weights indicate the probability of compatibility for each pair.

---

**Subprotocol 1**  $\text{matchHLA}(\langle \text{hla}_d \rangle^B: \text{vector}, \langle \text{ahla}_r \rangle^B: \text{vector}) \rightarrow \text{int}$

---

```

1:  $\langle \text{comp} \rangle^B \leftarrow \langle 0 \rangle^B \text{HLA}$ 
2: for  $i = 0, \dots, |\text{HLA}| - 1$  do ▷ SIMD
3:    $\langle \text{comp} \rangle^B[i] \leftarrow \langle \text{hla}_d[i] \rangle^B \wedge \langle \text{ahla}_r[i] \rangle^B$ 
4: end for
5:  $\langle \text{combined} \rangle^B \leftarrow \text{ORTREE}(\langle \text{comp} \rangle^B)[0]$ 
6: return  $\neg \langle \text{combined} \rangle^B$ 

```

---

We present the main protocols for the compatibility assessment in the following. The subprotocols for assessing the individual matching criteria HLA mismatches, ABO blood type, age, sex, and weight are given as Subprotocols 7 to 11 in the Appendix.

The HLA crossmatch is shown in Subprotocol 1. It tests whether the human leukocyte antigens of the donor are unsuitable to the human leukocyte antibodies of the recipient rendering them incompatible.

The subprotocol takes a vector with the antigens of a donor  $\text{hla}_d$  and a vector with the antibodies of the recipient  $\text{ahla}_r$  as input. The number of observed HLA, denoted by  $|\text{HLA}|$ , is publicly known. A vector

$\text{comp}$  stores whether the recipient possesses an antibody against any of the donor's HLA (cf. Line 3). For enhanced efficiency, we parallelize this comparison as *Single Instruction, Multiple Data* (SIMD) operation such that all HLA matches of one patient are computed in just one step. Afterwards, the overall compatibility (i.e., no antigen-antibody mismatch was found) is computed with an OR gates in a tree structure, to reduce the (multiplicative) depths of the circuit from  $|\text{HLA}|$  to  $\log_2(|\text{HLA}|)$ . To prepare for further processing, we invert combined and return it as result of the HLA crossmatching in Line 6.

---

**Protocol 2**  $\text{computeCompatibilityGraph}(\langle \text{pairs} \rangle^B: \text{vector}, \langle w \rangle^A: \text{vector}) \rightarrow \text{weighted adjacency matrix}$

---

```

1:  $\langle \text{compG} \rangle^A \leftarrow \text{matrix} \in \{ \langle 0 \rangle^A \}^{|\text{pairs}| \times |\text{pairs}|}$ 
2: for  $i = 0, \dots, |\text{pairs}| - 1$  do
3:   for  $j = 0, \dots, |\text{pairs}| - 1$  do
4:      $d \leftarrow \text{pairs}[i].d$  ▷ Extract donor.
5:      $r \leftarrow \text{pairs}[j].r$  ▷ Extract recipient.
6:      $\langle \text{edge.w} \rangle^A \leftarrow \langle 1 \rangle^A +$ 
        $\langle w \rangle^A[0] \cdot \text{b2a}(\text{evalHLA}(\langle d.\text{hla} \rangle^B, \langle r.\text{hla} \rangle^B)) +$ 
        $\langle w \rangle^A[1] \cdot \text{b2a}(\text{evalABO}(\langle d.\text{bg} \rangle^B, \langle r.\text{bg} \rangle^B)) +$ 
        $\langle w \rangle^A[2] \cdot \text{b2a}(\text{evalAge}(\langle d.\text{a} \rangle^B, \langle r.\text{a} \rangle^B)) +$ 
        $\langle w \rangle^A[3] \cdot \text{b2a}(\text{evalSex}(\langle d.\text{sex} \rangle^B, \langle r.\text{sex} \rangle^B)) +$ 
        $\langle w \rangle^A[4] \cdot \text{b2a}(\text{evalWeight}(\langle d.\text{weight} \rangle^B, \langle r.\text{weight} \rangle^B))$ 
7:      $\langle \text{compG} \rangle^A[i][j] \leftarrow$ 
        $\text{b2a}(\text{matchHLA}(\langle d.\text{hla} \rangle^B, \langle r.\text{ahla} \rangle^B) > \langle 0 \rangle^B ?$ 
        $\text{a2b}(\langle \text{edge.w} \rangle^A) : \langle 0 \rangle^B)$ 
8:   end for
9: end for
10: return  $\langle \text{compG} \rangle^A$ 

```

---

In Protocol 2, we present our MPC protocol that combines the results of the evaluated six medical criteria influencing the compatibility of a kidney donation into a weighted adjacency matrix indicating the donor-recipient compatibility, named  $\text{compG}$ .

It takes a vector  $\text{pairs}$  containing all possible pairs of donors and recipients and a vector  $w$  with a weight for each criteria (i.e., how much it influences the overall probability for good compatibility compared to the other factors) as input. Lines 4 to 6 additively combine the computed weighted probability of each compatibility criterion and assign it to the respective edge representing the donor of the  $i$ -th pair and the patient of the  $j$ -th pair, where  $i \neq j$  and  $i, j \in \{0, \dots, |\text{pairs}| - 1\}$ . In Line 7, we additionally check whether the  $i$ -th donor and the  $j$ -th patient exhibit general immunological compatibility using the HLA crossmatch subprotocol (cf. Subprotocol 1). If this is the case, we store the result of the edge weight at the respective index, otherwise we store the secret shared constant 0.

*MPC Cost.* The two sections in Subprotocol 1 evaluate  $|\text{HLA}|$  AND gates (as SIMD) and  $\log_2(|\text{HLA}|)$  OR<sup>[3]</sup> gates, respectively. Finally, we invert combined once.

---

<sup>[3]</sup>  $A \vee B = 1 \oplus ((1 \oplus A) \wedge (1 \oplus B))$



This results in a circuit depth of  $\log_2(|HLA|) + 1$  and a total number of AND gates of  $2 \times |HLA|$ . Boolean sharing ( $\mathcal{B}$ ) is used in this protocol, as Boolean operations are performed and the circuit depths is low, thanks to the SIMD vectorization [54].

To fully assess the matching quality (Protocol 2), all criteria have to be evaluated for each recipient, i.e., Protocols 1, 7, 9, 8, 10, and 11 are run  $|\text{pairs}|^2$  times. Then, in Protocol 2, we additionally evaluate five multiplications, five additions, one comparison, one AND gate, and one MUX gate. Due to the arithmetic operations in this protocol, the results of the compatibility evaluation protocols must be converted between  $\mathcal{B}$  and  $\mathcal{A}$ .

### Cycle Computation

The second phase of SPIKE computes the number of possible kidney exchange cycles given a concrete input cycle length<sup>[4]</sup> from the compatible donors and recipients that were output by the compatibility matching. Our MPC protocol for this part is shown in Protocol 3.

---

**Protocol 3** `determineNumberCycles( $\langle\text{compG}\rangle^{\mathcal{A}}$ : matrix)  $\rightarrow$  number of cycles`

---

```

 $\langle\text{compG}\rangle^{\mathcal{B}} \leftarrow \text{a2b}(\langle\text{compG}\rangle^{\mathcal{A}})$ 
 $\langle\text{uG}\rangle^{\mathcal{A}} \leftarrow \text{removeWeights}(\langle\text{compG}\rangle^{\mathcal{B}})$ 
 $\langle\text{cG}\rangle^{\mathcal{A}} \leftarrow \text{pow}(\langle\text{uG}\rangle^{\mathcal{A}}, \text{cLen})$ 
 $\langle\text{cycles}\rangle^{\mathcal{A}} \leftarrow \langle 0 \rangle^{\mathcal{A}}$ 
for  $i = 0, \dots, |\text{pairs}| - 1$  do
   $\langle\text{cycles}\rangle^{\mathcal{A}} \leftarrow \langle\text{cycles}\rangle^{\mathcal{A}} + \langle\text{cG}\rangle^{\mathcal{A}}[i][i]$ 
end for
return  $\langle\text{cycles}\rangle^{\mathcal{A}}$ 

```

---

Protocol 3 takes the secret shared weighted compatibility graph `compG` as input. The desired length of cycles `cLen` is public. We first compute the unweighted adjacency matrix in Line 2 (cf. Subprotocol 12, in the Appendix). For the unweighted matrix, we compute the `cLen`-th power using a naïve implementation<sup>[5]</sup>. The entries in this resulting matrix indicate how many paths of length `cLen` start at vertex  $i$  and end at vertex  $j$ . For cycles, the entries are on the diagonal, as start and end vertex are identical. Following this thought, the sum of the entries of the diagonal is the total number of cycles with the given cycle length `cLen`. Note that this number contains duplicates, namely, “congruent” cycles that are the same but were found via a

<sup>[4]</sup>As discussed in the Related Work, we recommend 2 to 3 to foster robustness.

<sup>[5]</sup>Even though exhibiting a cubic runtime complexity, this part’s performance is negligible compared to the following parts (cf. Figure 4), hence, an optimization is not vital.

different start/end vertex.<sup>[6]</sup> We remove the duplicates later in Subprotocol 14 (described in the Appendix). *MPC Cost.* Protocol 3 contains mostly arithmetic operations ( $|\text{pairs}|^3$  multiplications and  $(|\text{pairs}|^3 - |\text{pairs}|^2)$  additions), however, the computation of the unweighted adjacency matrix is most efficiently performed in  $\mathcal{B}$   $|\text{pairs}|^2$  comparisons and MUX gates). For that reason we convert `compG` from  $\mathcal{A}$  to  $\mathcal{B}$  (cf. Line 1) and back (in Protocol 12).

---

**Subprotocol 4** `findCycles( $\langle\text{compG}\rangle^{\mathcal{B}}$ : matrix,  $\text{cCycle}$ : vector,  $\langle\text{allCycles}\rangle^{\mathcal{B}}$ : vector,  $\langle\text{weight}\rangle^{\mathcal{B}}$ : int,  $\langle\text{valid}\rangle^{\mathcal{B}}$ : int)  $\rightarrow$  vector of tuples`

---

```

1: if  $|\text{cCycle}| == \text{cLen}$  then
2:    $\langle\text{weight}\rangle^{\mathcal{B}} \leftarrow \langle\text{weight}\rangle^{\mathcal{B}} + \langle\text{compG}\rangle^{\mathcal{B}}[\text{cLen} - 1][0]$ 
3:    $\langle\text{valid}\rangle^{\mathcal{B}} \leftarrow \langle\text{compG}\rangle^{\mathcal{B}}[\text{cLen} - 1][0] > \langle 0 \rangle^{\mathcal{B}} ?$ 
      $\langle\text{valid}\rangle^{\mathcal{B}} + \langle 1 \rangle^{\mathcal{B}} : \langle\text{valid}\rangle^{\mathcal{B}} + \langle 0 \rangle^{\mathcal{B}}$ 
4:    $\langle\text{addC}\rangle^{\mathcal{B}} \leftarrow \langle\text{cLen}\rangle^{\mathcal{B}} == \langle\text{valid}\rangle^{\mathcal{B}}$ 
5:    $\langle\text{cWeight}\rangle^{\mathcal{B}} \leftarrow \langle\text{addC}\rangle^{\mathcal{B}} ? \langle\text{weight}\rangle^{\mathcal{B}} : \langle 0 \rangle^{\mathcal{B}}$ 
6:    $\langle\text{cycle}\rangle^{\mathcal{B}} \leftarrow \langle\text{cCycle}\rangle^{\mathcal{B}}$ 
7:    $\langle\text{allCycles}\rangle^{\mathcal{B}}.\text{append}(\langle\langle\text{cWeight}\rangle^{\mathcal{B}}, \langle\text{cycle}\rangle^{\mathcal{B}}\rangle)$ 
8:   revert()
9: else
10:  for  $i = 0, \dots, |\text{pairs}| - 1$  do
11:    if  $\text{cCycle.contains}(i)$  then
12:      continue
13:    else
14:       $\langle\text{weight}\rangle^{\mathcal{B}} \leftarrow \langle\text{weight}\rangle^{\mathcal{B}} + \langle\text{compG}\rangle^{\mathcal{B}}[-1][i]$ 
15:       $\langle\text{valid}\rangle^{\mathcal{B}} \leftarrow \langle\text{compG}\rangle^{\mathcal{B}}[-1][0] > \langle 0 \rangle^{\mathcal{B}} ?$ 
         $\langle\text{valid}\rangle^{\mathcal{B}} + \langle 1 \rangle^{\mathcal{B}} : \langle\text{valid}\rangle^{\mathcal{B}} + \langle 0 \rangle^{\mathcal{B}}$ 
16:       $\text{cCycle.append}(i)$ 
17:       $\langle\text{allCycles}\rangle^{\mathcal{B}} \leftarrow \text{findCycles}(\langle\text{compG}\rangle^{\mathcal{B}},$ 
         $\text{cCycle}, \langle\text{allCycles}\rangle^{\mathcal{B}}, \langle\text{weight}\rangle^{\mathcal{B}}, \langle\text{valid}\rangle^{\mathcal{B}})$ 
18:       $\text{cCycle.remove}()$ 
19:      revert()
20:    end if
21:  end for
22: end if
23: return  $\langle\text{allCycles}\rangle^{\mathcal{B}}$ 

```

---

### Cycle Evaluation

The third phase of SPIKE then identifies the most likely successful unique exchange cycles consisting of compatible pairs of donors and recipients.

Our first subprotocol for this phase, shown in Subprotocol 4, finds all exchange cycles of the desired length (including duplicates) and computes the weight of each cycle. This weight is the sum of all included weighted edges. As mentioned before, the weight associated with an exchange cycle indicates the probability of the transplantation being successfully carried out, i.e., its robustness.

The subprotocol takes the secret shared compatibility graph `compG` output by Protocol 2, the currently analyzed exchange cycle `cCycle`, its secret shared weight `weight`, a secret shared counter `valid` which

<sup>[6]</sup>Cycle (A, B, C) and cycle (B, C, A) are duplicates, but cycle (C, B, A) is not.

tracks the number of edges in  $cCycle$ , and a vector of secret shared tuples  $allCycles$  which will be consecutively filled with all possible exchange cycles and the corresponding sum of weights. In a recursive execution of Subprotocol 4, this vector is filled as explained in detail in the following. The desired output cycle length  $cLen$  and the number of recipient-donor pairs  $|pairs|$  are public. Additionally, also the output number of cycles  $|cycles|$  found in Protocol 3 is revealed for efficiency reasons. We consider this leakage as acceptable since it leaks only a very high-level aggregate property, generally not allowing the inference of the compatibility graph's topology<sup>[7]</sup>.

Subprotocol 4 first checks if the currently analyzed exchange cycle  $cCycle$  already has the desired length  $cLen$ . If this is the case, the weight of the last edge is added to the respective sum of this cycle's weights in Line 2. Next, each valid  $cCycle$  is added to  $allCycles$  with its respective sum of weights. A  $cCycle$  is valid, if it is closed (cf. Lines 3 to 4). An invalid cycle is associated with weight zero (cf. Line 5). Note that a weight of zero does not contribute to the solution, hence a cycle with weight zero is never considered for a solution. In Line 8, the operations done in Lines 2 to 3 are reverted to restore the state of  $cCycle$  before the last edge was added, i.e., the weight of the last edge is subtracted from  $weight$  and  $valid$  is decreased by 0 (no edge) or 1 (edge).

Cycles that do not have the desired length yet are handled in Lines 10 to 21. For these exchange cycles, the subprotocol checks whether they are already part of  $cCycle$  as each vertex may only appear at most once (cf. Line 11). If it is not included, the weight of the edge from the previous to the new vertex is added by increasing  $cCycle$ 's weight and counter  $\langle valid \rangle^{\mathcal{Y}}$ , and the new vertex is added to  $cCycle$  (cf. Lines 14 to 16). Afterwards, Subprotocol 4 is recursively called again with the newly added vertex. Once the function returns, we revert the operations done before to be able to analyze the next cycle (cf. Lines 18 to 19).

The second subprotocol of the cycle evaluation (cf. Subprotocol 14 in the Appendix) removes duplicates from the exchange cycles set. It extracts  $\#unique = \lfloor \frac{\#cycles}{cLen} \rfloor$  cycles and returns the  $k$  cycles with the highest probability for a successful transplantation.

<sup>[7]</sup>Exceptions are fully connected and unconnected graphs, as well as for  $|cycles| = 1$  at pathological graph topologies. The first topologies have no security implication whatsoever and the later can, e.g., be easily avoided by introducing a check ensuring that the output is only revealed when more cycles have been found.

---

**Protocol 5**  $evaluateCycles(\langle compG \rangle^{\mathcal{Y}}: matrix) \rightarrow$   
vector of tuples

---

```

1:  $\langle allCycles \rangle^{\mathcal{Y}}, cCycle \leftarrow \emptyset$ 
2:  $\langle weight \rangle^{\mathcal{Y}}, \langle valid \rangle^{\mathcal{Y}} \leftarrow \langle 0 \rangle^{\mathcal{Y}}$ 
3: for  $i = 0, \dots, |pairs| - 1$  do
4:    $cCycle.append(i)$ 
5:    $\langle allCycles \rangle^{\mathcal{Y}} \leftarrow findCycles(\langle compG \rangle^{\mathcal{Y}}, cCycle,$ 
      $\langle allCycles \rangle^{\mathcal{Y}}, \langle weight \rangle^{\mathcal{Y}}, \langle valid \rangle^{\mathcal{Y}})$ 
6:    $cCycle.remove()$ 
7: end for
8:  $|allCycles| \leftarrow totalCycles()$ 
9:  $\langle sortedCycles \rangle^{\mathcal{Y}} \leftarrow kNNSort(\langle allCycles \rangle^{\mathcal{Y}}, |cycles|)$ 
10:  $|unique| \leftarrow \lfloor \frac{|cycles|}{cLen} \rfloor$ 
11:  $\langle filteredCycles \rangle^{\mathcal{Y}} \leftarrow removeDuplicates(\langle sortedCycles \rangle^{\mathcal{Y}})$ 
12: return  $\langle filteredCycles \rangle^{\mathcal{Y}}$ 

```

---

Protocol 5 combines the previously discussed subprotocols. It first calculates the sum of weights for each cycle with Subprotocol 4 ( $findCycles$ ) and sorts the result using Subprotocol 13 ( $kNNSort$ ) such that only the  $k$  cycles with the largest weight are output. Those are all valid cycles, possibly including duplicates. Afterwards, the protocol removes all duplicates within the  $k$  cycles.

*MPC Cost.* The complexity of Subprotocol 4 depends on the number of pairs  $|pairs|$ ,  $cLen$ , and the number of possible cycles  $|allCycles|$ . It is most efficient in  $\mathcal{Y}$  as the MUX gates are not independent, thus, creating a deep circuit of depth  $\mathcal{O}(|allCycles| \times |cycles| \times cLen)$ . For removing duplicates and extracting the most robust  $k$  exchange circuits, we evaluate  $\#cycles \times (\#unique + \sum_{i=0}^{\#cycles} (cLen \times (cLen - 1)))$  comparisons,  $\#cycles \times \sum_{i=0}^{\#cycles} ((cLen \times (cLen - 1)))$  AND gates,  $\#cycles \times \sum_{i=0}^{\#cycles} (cLen - 1)$  OR gates,  $\#cycles \times \#unique \times (1 + cLen) + \#cycles$  MUX gates. This step is most efficient with  $\mathcal{Y}$  as the circuit is very deep. Thus, the complete cycle evaluation routine is most efficient in  $\mathcal{Y}$  as each of our subroutines is most efficient in  $\mathcal{Y}$ .

#### Solution Evaluation

The fourth phase of SPIKE determines the final output, a set of *disjoint* exchange cycles exhibiting the highest probability for a successful transplantation. As a pair of donor and recipient can only be involved in one exchange cycle, the output sets must be vertex disjoint. Note that we find a locally optimal solution which might differ from the globally optimal solution<sup>[8]</sup>. This last part of SPIKE is shown in Protocol 6.

Protocol 6 takes a secret shared vector of tuples  $filteredCycles$  with all valid unique cycles and their respective weights, the number of valid cycles  $|unique|$ , and the cycle length  $cLen$  as input. The number of pairs  $|pairs|$  is a public variable as before.

<sup>[8]</sup>Calculation of a global solution is provably a  $\mathcal{NP}$ -hard problem [59].

---

**Protocol 6** evalSolution( $\langle\text{filteredCycles}\rangle^{\mathcal{Y}}$ : vector of tuples)  $\rightarrow$  tuple(int, vector of vectors)

---

```

1:  $\langle\text{sets}\rangle^{\mathcal{Y}} \leftarrow \emptyset$ 
2:  $\langle\text{weights}\rangle^{\mathcal{Y}} \leftarrow \emptyset$ 
3:  $\langle\text{dummyC}\rangle^{\mathcal{Y}} \leftarrow \{\langle\text{pairs}\rangle^{\mathcal{Y}}\}^{\text{cLen}}$ 
4: for  $i = 0, \dots, |\text{unique}| - 1$  do
5:    $\langle\text{tempSet}\rangle^{\mathcal{Y}} \leftarrow \emptyset$ 
6:    $\langle\text{tempSet}\rangle^{\mathcal{Y}}.\text{append}(\langle\text{filteredCycles}\rangle^{\mathcal{Y}}[i][1])$ 
7:    $\langle\text{weight}\rangle^{\mathcal{Y}} \leftarrow \langle\text{filteredCycles}\rangle^{\mathcal{Y}}[i][0]$ 
8:    $\text{counter} \leftarrow 1$ 
9:   for  $j = 0, \dots, |\text{unique}| - 1$  do
10:    if  $i == j$  then
11:      continue
12:    end if
13:     $\langle\text{cCycle}\rangle^{\mathcal{Y}} \leftarrow \langle\text{filteredCycles}\rangle^{\mathcal{Y}}[j][1]$ 
14:     $\langle\text{disjoint}\rangle^{\mathcal{Y}} \leftarrow \text{disjointSet}(\langle\text{tempSet}\rangle^{\mathcal{Y}},$ 
15:       $\langle\text{cCycle}\rangle^{\mathcal{Y}})$ 
16:     $\langle\text{vertices}\rangle^{\mathcal{Y}} \leftarrow \emptyset$ 
17:     $\langle\text{vertices}\rangle^{\mathcal{Y}}.\text{append}(\langle\text{disjoint}\rangle^{\mathcal{Y}} ?$ 
18:       $\langle\text{cCycle}\rangle^{\mathcal{Y}} : \langle\text{dummyC}\rangle^{\mathcal{Y}})$ 
19:     $\langle\text{weight}\rangle^{\mathcal{Y}} \leftarrow \langle\text{disjoint}\rangle^{\mathcal{Y}} ? \langle\text{weight}\rangle^{\mathcal{Y}} : \langle 0 \rangle^{\mathcal{Y}}$ 
20:     $\langle\text{tempSet}\rangle^{\mathcal{Y}}.\text{append}(\langle\text{vertices}\rangle^{\mathcal{Y}})$ 
21:     $\text{counter} \leftarrow \text{counter} + 1$ 
22:  end for
23:  $\langle\text{sets}\rangle^{\mathcal{Y}}.\text{append}(\langle\text{tempSet}\rangle^{\mathcal{Y}})$ 
24:  $\langle\text{weights}\rangle^{\mathcal{Y}}.\text{append}(\langle\text{weight}\rangle^{\mathcal{Y}})$ 
25: end for
26: return findMaximumSet( $\langle\text{sets}\rangle^{\mathcal{Y}}, \langle\text{weights}\rangle^{\mathcal{Y}}$ )

```

---

It checks each valid cycle  $\text{cCycle}$  if it is disjoint from all other previously analyzed cycles in  $\text{tempSet}$ . The MPC subprotocol for testing the disjointness is given in Subprotocol 16 in the Appendix. If it is disjoint,  $\text{cCycle}$  is added to the set of potential solutions (Lines 16 - 22). Finally, the set with the highest weight is returned. Details of the corresponding MPC protocol can be found in Subprotocol 17 in the Appendix.

*MPC Cost.* In total, we evaluate  $|\text{unique}|^2$  ADD gates,  $|\text{unique}|^2 \times \text{cLen} + |\text{unique}|$  comparisons,  $4 \times |\text{unique}|^2 + |\text{unique}|$  MUX, and  $|\text{unique}|^2 \times \text{cLen}^2$  OR gates. The solution evaluation is most efficient in  $\mathcal{Y}$  as there are only few arithmetic operations and mostly comparisons.

### Complexity Assessment

In Table 4, the asymptotic complexities for the four phases of SPIKE are given.

The most important parameters of the first part, the Compatibility Matching shown in the first section of the table, are the number of HLA (cf. Background)  $|\text{HLA}|$  and the number of pairs  $|\text{pairs}|$ . In the default configuration,  $|\text{HLA}|$  is 50. For the second phase, the dominant parameter is the number of pairs  $|\text{pairs}|$ . In the third section of Table 4, the asymptotic complexity for the Cycle Evaluation is given. The relevant parameters here are the number of pairs  $|\text{pairs}|$ , the total number of cycles  $|\text{allCycles}| = |\text{pairs}|^{\text{cLen}}$ , the number of existing cycles  $|\text{cycles}|$ , the number of unique cycles  $|\text{unique}| = \lfloor \frac{|\text{cycles}|}{\text{cLen}} \rfloor$ , the length of cycles  $\text{cLen}$ , and the

factor  $k$  (i.e, the number of cycles with highest probability for successful transplantation), and the number of elements in  $\text{cyclesSet}$ ,  $|\text{cyclesSet}|$  of Protocol 13. The most important parameters of the last phase, the Solution Evaluation, are the number of unique cycles  $|\text{cycles}|$ , and the length of cycles  $\text{cLen}$ .

Overall, the asymptotic complexity of SPIKE is:

$$\mathcal{O}(|\text{pairs}|^2 \times |\text{HLA}| + \text{cLen} \times |\text{pairs}|^3 + |\text{cycles}|^3 \times \text{cLen}^2).$$

The most most important parameters are the number of pairs  $|\text{pairs}|$ , the number of considered HLA  $|\text{HLA}|$ , the length of cycles  $\text{cLen}$ , and the number of unique cycles  $|\text{cycles}|$ .

## Results

All benchmarks were run on two servers equipped with Intel Core i9-7960X processors and 128 GB RAM. They are connected via 10 Gb/s LAN with a median latency of 1.3 ms. All benchmarks are averaged over 10 runs.

### Network Setups

To provide meaningful performance benchmarks for a variety of real-world settings, we envision two network settings for privacy-preserving KEP that we describe in the following. In addition, for the comparison to the works of Breuer et al. [8, 9], we replicated their network setting with 1 Gb/s bandwidth and 1 ms of latency.

*LAN.* The high-bandwidth, low latency network scenario, here referred to as *LAN*, is the most relevant real-world scenario for our application. In Germany, most (larger) medical institutions utilize high-bandwidth Internet connections. In the case of most university hospitals the German Research Network (“Deutsches Forschungsnetz” DFN<sup>[9]</sup>) provides dedicated, high bandwidth communication networks. Our *LAN* benchmarks are performed using a 10 Gb/s connection with an average latency of 1.3 ms.

*WAN.* One benefit of a MPC-based privacy-preserving KEP solution could be reduced legal and regulatory data protection requirements, due to the high security level of the computation itself. This would allow smaller, local hospitals and medical practices to directly participate in the kidney exchange. Those institutions might be connected via residential Internet access. For that scenario, we benchmarked SPIKE in a reduced-bandwidth, high latency network. A bandwidth restriction to 100 Mb/s with added latency of 100 ms was implemented using the `tc`<sup>[10]</sup> command to simulate the *WAN* network. The high latency was chosen to take packet loss due to unreliable connections into account.

<sup>[9]</sup><https://dfn.de/>

<sup>[10]</sup><https://man7.org/linux/man-pages/man8/tc.8.html>

**Table 4** Complexity Assessment

Phase	Name	Protocol	Time Complexity
Part 1)	Compatibility Matching	Subprotocol 1	$\mathcal{O}( HLA )$
		Subprotocol 7	$\mathcal{O}( HLA )$
		Subprotocol 8	$\mathcal{O}(1)$
		Subprotocol 9	$\mathcal{O}(1)$
		Subprotocol 10	$\mathcal{O}(1)$
		Subprotocol 11	$\mathcal{O}(1)$
		Protocol 2	$\mathcal{O}( pairs ^2 \times  HLA )$
Part 2)	Cycle Computation	Subprotocol 12	$\mathcal{O}( pairs ^2)$
		Protocol 3	$\mathcal{O}(cLen \times  pairs ^3)$
Part 3)	Cycle Evaluation	Subprotocol 15	$\mathcal{O}(1)$
		Subprotocol 4	$\mathcal{O}( pairs ^{cLen})$
		Subprotocol 13	$\mathcal{O}( cyclesSet  \times k \times cLen)$
		Subprotocol 14	$\mathcal{O}( cycles ^2)$
		Protocol 5	$\mathcal{O}( pairs ^{cLen})$
Part 4)	Solution Evaluation	Subprotocol 16	$\mathcal{O}( cycles  \times cLen)$
		Subprotocol 17	$\mathcal{O}( cycles ^2)$
		Protocol 6	$\mathcal{O}( cycles ^3 \times cLen^2)$

### Performance Benchmarks

Figure 3 shows the total runtime of SPIKE for varying numbers of pairs, both network settings, and cycle lengths  $L = 2$  and  $L = 3$ . The full results are in Tables 6 to 11 in the Appendix.

During the evaluation of longer cycles ( $L \geq 3$ ) RAM utilization proved itself to be a bottleneck for execution. For those scenarios, we benchmarked up to RAM exhaustion and extrapolated the runtimes according to the underlying power-law complexity. The extrapolation is shown with a dashed line. The sudden increase in runtime for  $L = 3$  between 12 and 13 pairs occurs due to swapping.

As a general result, the expected polynomial relationship between the number of pairs and the overall runtime can be observed, reflected in the power-law development in the semilog graphs. For  $L = 2$ , we achieve a total runtime of under 4 min for 40 pairs, thus, demonstrating real-world applicable performance. The WAN setting increases the overall runtime by less than an order of magnitude. Calculation times under 20 min for 40 pairs in this setting render the participation feasible for physicians with residential Internet connections. To find a solution for larger cycle lengths, the exponent in the time complexity increases, increasing the runtimes significantly. But even then 25 pairs are computable in around 1 h.

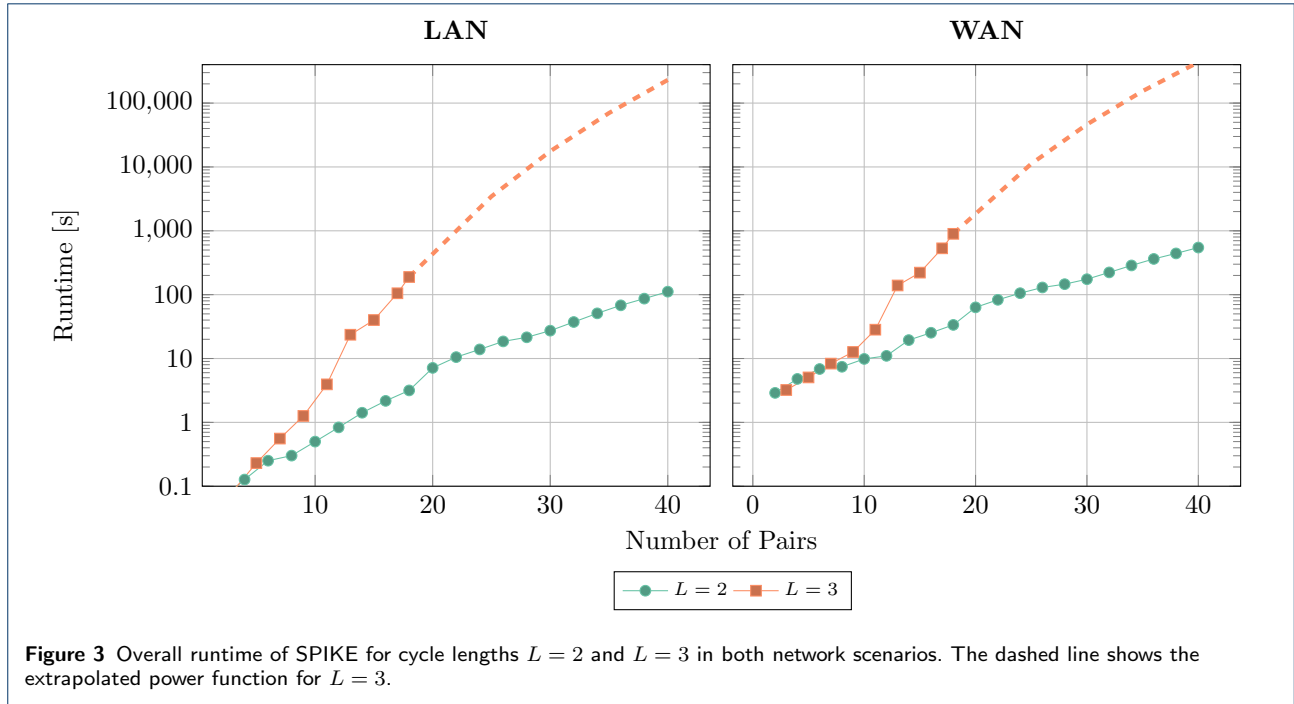
Figure 4 shows the runtimes of the individual parts of the algorithm ( $L = 2$ ). It is clearly visible, that the medical compatibility testing and graph creation, as well as the cycle computation quickly become negligible compared to the runtimes of cycle evaluation and the evaluation of the global solution. The duration of online and offline phases are in the same order of magnitude. By executing the phases separately, a 134% performance increase in the online execution can be

achieved, compared to the accumulated runtime (cf. Figure 3).

### Comparison to State-Of-The-Art

In Figure 5, we compare the runtime of our implementation for  $L = 2$  and  $L = 3$  with two implementations from Breuer *et al.* [8, 9]. The first implementation [8] uses a Threshold Homomorphic Encryption scheme and enables to solve the privacy-preserving KEP with arbitrary cycle length as in SPIKE. The maximum cycle size is set to  $L = 3$  in their benchmarks. The second one [9] is based on three-party honest majority Shamir’s Secret Sharing using the MP-SPDZ framework and limits its cycle length to  $L = 2$ . The performance data for both implementations is taken from the referenced publications.

Our implementation, as well as the MP-SPDZ based state-of-the-art [9], shows a polynomial-bound power-law graph. The Homomorphic Encryption-based implementation shows clearly an exponential runtime development, increasing rapidly. For 9 pairs, the maximum number of pairs benchmarked in the original publication [8], our implementation achieves a 29 828 × speedup. For  $L = 2$ , our implementation performs 414 × better than the MP-SPDZ-based implementation [9]. To improve the medical quality of the donor-recipient matching, we implemented additional matching criteria, as described in the “Background” section. As we have seen in Figure 4, the performance impact of the compatibility matching algorithm is negligible compared to the runtime of the remaining algorithmic parts. However, in Figure 6 we compare the performance difference between the reduced set of medical matching criteria and the full set. For small number of pairs there is a transient phase, where the runtime of the full set rises faster. After this transient phase, both curves assume nearly the same slope. In the plots for



the WAN network model, the latency-induced “baseline” runtime can be observed.

## Discussion

### Security Guarantees

Our privacy-preserving kidney exchange protocol, SPIKE, is implemented using the ABY [54] MPC framework, guaranteeing computational semi-honest security in a two-party setting. An adversary  $\mathcal{A}$  can corrupt at most one of the two computing parties.  $\mathcal{A}$  is assumed to follow the protocol specification and gets access to all messages of the corrupted party (sent and received) while trying to extract private information. This security model is standard in the privacy research community and protects against two security concerns: 1. inadvertent disclosure of sensitive data and 2. *full* data disclosure in case of a breach in one of the parties (in comparison to a centralized computation). In the outsourcing scenario with two computation parties and an arbitrary number of data sources, both computation parties *must not* collude. However, an arbitrary number of data sources is allowed to collude or behave maliciously, without breaking the security guarantees. Note, that MPC only gives privacy guarantees for the computation, whereas maliciously formed inputs might lead to incorrect outputs. For a “holistic” data privacy perspective, please see [60].

While this adversarial model is not sufficient for all applications, e.g., computations with parties in different jurisdictions [61], it suits our intended set-

ting, namely the joint computation among large, intra-national medical institutions. Both semi-honest behaviour as well as the non-collusion assumption can be enforced by legal and regulatory means.

For a full description of the cryptographic assumptions and guarantees inherited by the primitives used in ABY, we refer to the respective section in the Appendix and the original ABY publication [54].

While all  $s$ ' data, including the association to the various data sources are considered to be private data and are protected by the aforementioned guarantees, we consider the *number* of donor-recipient pairs, as well as the maximum number of cycles in the graph as public information. This choice has important performance impacts, however, if the numbers of pairs are to be considered private as well, the real numbers can be hidden by padding each input array to a fixed length with dummy entries.

### Real-World Deployability

This work introduces a protocol for finding a solution for the kidney exchange problem in a privacy-preserving fashion. As demonstrated in the performance benchmarks and the security discussion, it meets all initially determined requirements for a secure privacy-preserving KEP w.r.t privacy, efficiency, decentralization, and adaptability for medical experts.

Concretely, it enables real-world periodic batch-processing of a large number of donor-recipient pairs and a practical cycle length of  $L = 3$ , even in residential network settings. This allows even residential

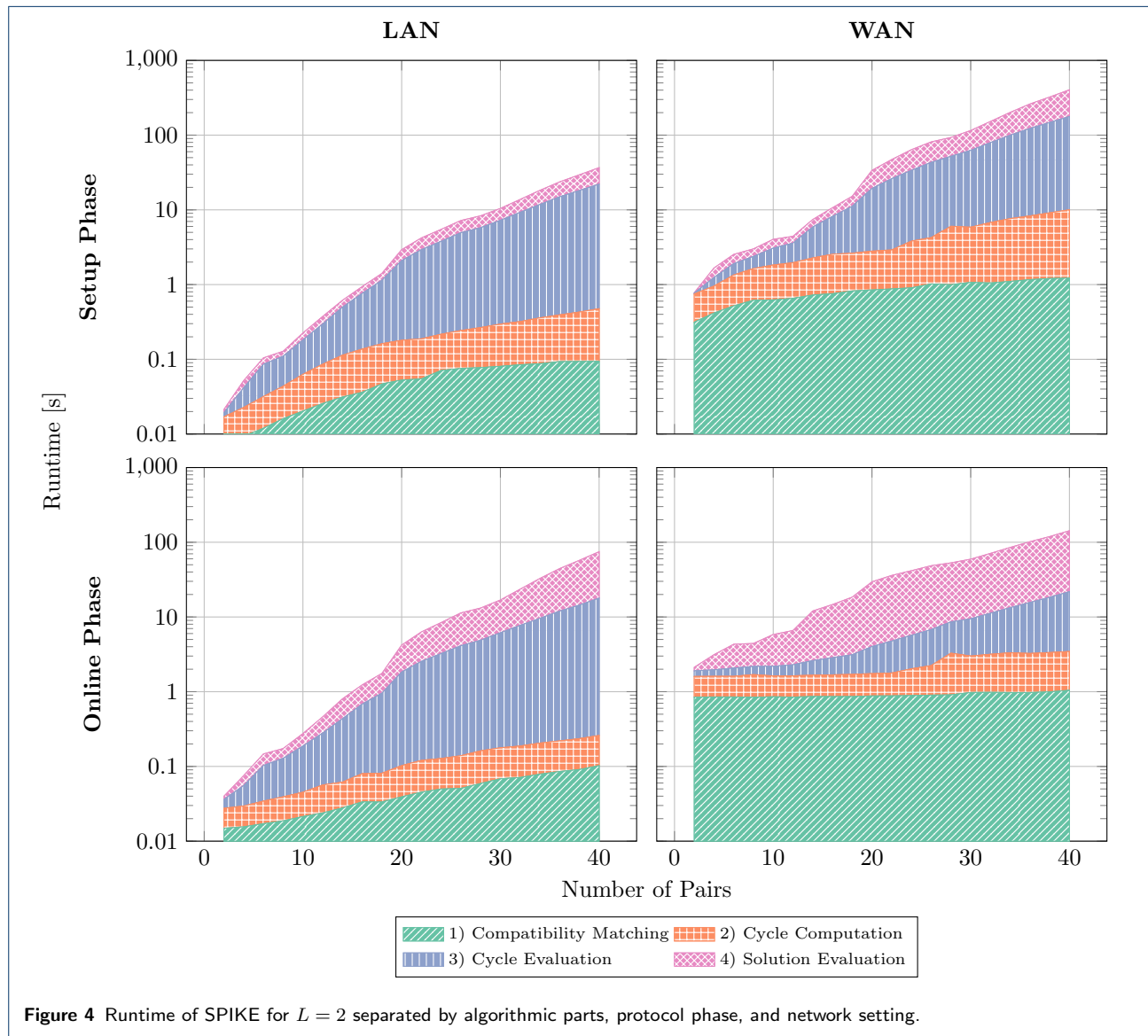
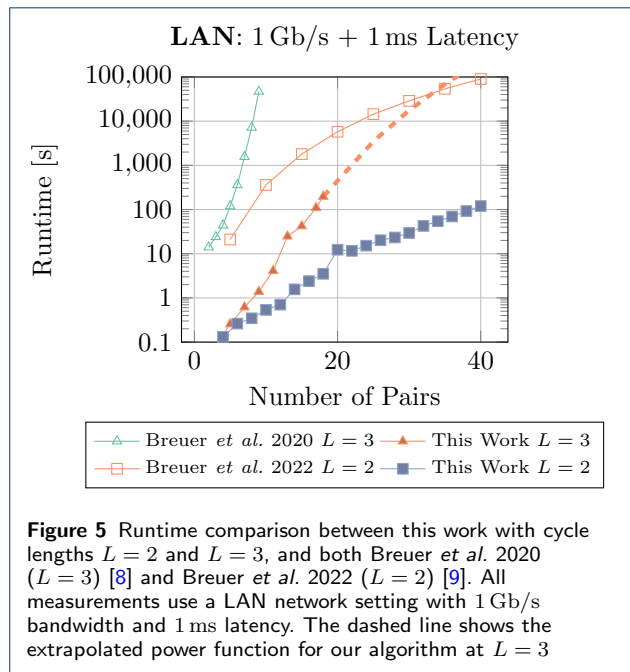


Figure 4 Runtime of SPIKE for  $L = 2$  separated by algorithmic parts, protocol phase, and network setting.



nephrology experts to participate in kidney exchanges, hence, providing a better medical care for their patients. However, SPIKE requires a significant amount of communication, thus, it is not yet ready for the usage of metered or cell data connections in a two-party computation protocol<sup>[11]</sup> which might be an interesting direction for future work.

By using state-of-the-art provably secure cryptographic techniques, the privacy of sensitive medical information of donors and recipients is fully protected by clearly defined hardness assumptions of mathematical problems. Furthermore, by pursuing a completely decentralized approach without a trusted third party, the risk of data leakages in case of a data security incident at one participating facility is significantly reduced, compared to a breach in a central computation node or repository.

Allowing medical professionals to choose many parameters of the algorithm to adapt to new evidence-based guidelines or specific situational constraints ensures flexibility and maintainability for future application. The compatibility matching algorithm is configurable by choosing the considered HLA, as well as the weights of the chosen medical factors. This explicitly allows the deactivation of chosen comparisons. Due to the clear architecture boundaries in the open source

<sup>[11]</sup>In contrast, SPIKE is already practical for an outsourcing scenario where mobile clients secret share their data among two non-colluding servers or cloud entities.

implementation, additional checks and criteria can easily be included.

While meeting all formal requirements, SPIKE falls short in two aspects: first, we observe a high memory consumption during the computation. This is expected, as this protocol was optimized for runtime performance. Additionally, hardware costs are, generally speaking, no hindrance for meeting data protection regulation. Thus, this aspect does not jeopardize the adoption in the intended use cases. However, developing internal batch processing of graph clusters and the employment of space-optimized data structures might be worthwhile opportunities for further research. An interesting direction for future work can be to explore the compatibility with recent advances in MPC-based graph analysis for breadth-first search [62] scaling linearly in the number of vertices. Second, the developed software components are research artifacts and fulfil a prototypical function. For real-world adoption the implementation of widespread medical standards, e.g., HL7 FHIR R4<sup>[12]</sup>, audit- and authentication capabilities, integration in medical research pipelines, creation of deployment packages, and lastly full (legal) documentation must be pursued. This is, however, not in the scope of this work.

## Conclusion

In this work, we introduced SPIKE, an efficient privacy-preserving Kidney Exchange Problem (KEP) protocol. Using provably secure cryptographic techniques, SPIKE provides highest data protection guarantees for patients' sensitive medical data, while allowing a decentralized computation of a solution to the kidney exchange problem. We implement adaptable medical compatibility matching algorithms, giving medical professionals the flexibility to accommodate updated guidelines and the specific situational constraints.

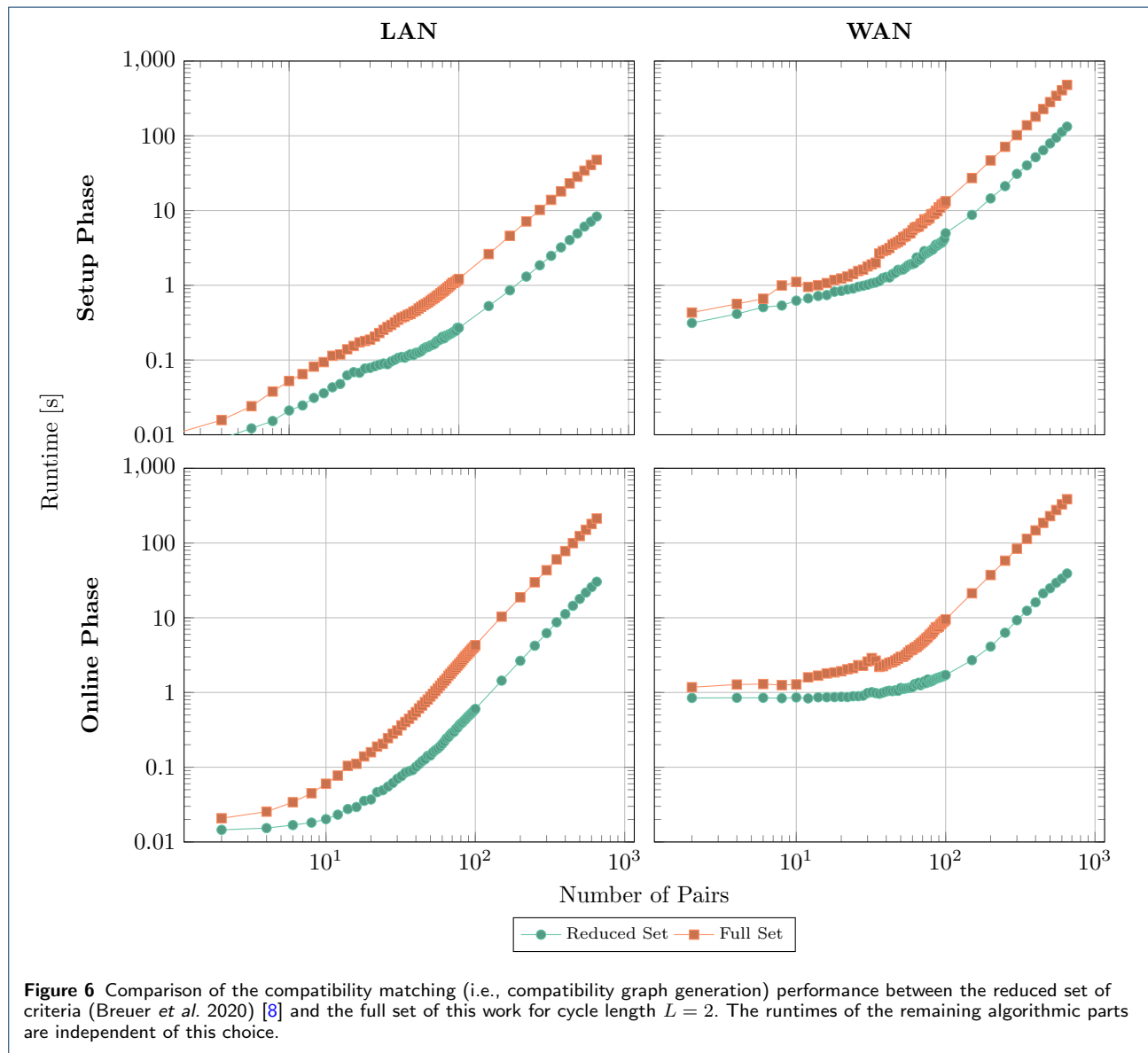
Our optimized protocols achieve a 30 000× and 400× speedup compared to the current state-of-the-art [8, 9] for cycle lengths of  $L = 3$  and  $L = 2$ , respectively. With a total runtime of under 4 min for 40 pairs at  $L = 2$  and around 1 h for 25 pairs at  $L = 3$ , we demonstrate feasible performance for many real-world applications.

We hope that the advancements in privacy protection and application performance will allow more medical facilities to participate in Kidney Exchanges, thus increasing the recipients' chances for timely and potentially live-saving surgery.

## Acknowledgements

Many thanks to Ulrich Zwirner for sharing his medical knowledge during our fruitful discussions.

<sup>[12]</sup><https://www.hl7.org/fhir/R4/>





### Funding

This project received funding from the European Research Council (ERC) under the European Union's Horizon 2020 research and innovation program (grant agreement No.850990 PSOTI). It was co-funded by the Deutsche Forschungsgemeinschaft (DFG) – SFB1119 CROSSING/236615297 and GRK2050 Privacy & Trust/251805230, by the German Federal Ministry of Education and Research and the Hessen State Ministry for Higher Education, Research and the Arts within ATHENE, and by the German Federal Ministry of Education and Research within the HiGHmed project (#01ZZ1802G).

### Abbreviations

MPC: Secure Multi-Party Computation; HE: Homomorphic Encryption; SSS: Shamir's Secret Sharing;  $\mathcal{Y}$ : Yao's Garbled Circuits;  $\mathcal{B}$ : Boolean Secret Sharing;  $\mathcal{A}$ : Arithmetic Secret Sharing; PPKE: Privacy-Preserving Kidney Exchange; KEP: Kidney Exchange Problem; HLA: Human Leukocyte Antigens

### Availability of data and materials

Our code and the datasets analyzed are available here: <https://encrypto.de/code/PPKE>.

### Ethics approval and consent to participate

Not applicable.

### Competing interests

The authors declare that they have no competing interests.

### Consent for publication

Not applicable.

### Authors' contributions

TB implemented the discussed software.  
TB and TK specified the medical requirements.  
HM and TK designed the research project and guided the protocol design.  
TB, TK, and HM designed the performance benchmarks which were conducted and analyzed by TB and TK.  
TS and KH led this research project.  
All authors contributed to the manuscript and substantively revised it. All authors read and approved the final manuscript.

### Author details

<sup>1</sup>ENCRYPTO, Technical University of Darmstadt, Darmstadt, Germany.

<sup>2</sup>Computational Biology & Simulation group, Technical University of Darmstadt, Darmstadt, Germany.

### References

- Murphy, D., McCulloch, C.E., Lin, F., Banerjee, T., Bragg-Gresham, J.L., Eberhardt, M.S., Morgenstern, H., Pavkov, M.E., Saran, R., Powe, N.R., Hsu, C.-y., for the Centers for Disease Control and Prevention Chronic Kidney Disease Surveillance Team: Trends in Prevalence of Chronic Kidney Disease in the United States. *Annals of Internal Medicine* **165**(7) (2016)
- Thurlow, J.S., Joshi, M., Yan, G., Norris, K.C., Agodoa, L.Y., Yuan, C.M., Nee, R.: Global Epidemiology of End-Stage Kidney Disease and Disparities in Kidney Replacement Therapy. *American Journal of Nephrology* **52**(2) (2021)
- Ibrahim, H.N., Foley, R., Tan, L., Rogers, T., Bailey, R.F., Guo, H., Gross, C.R., Matas, A.J.: Long-Term Consequences of Kidney Donation. *The New England Journal of Medicine* (2009)
- Eurotransplant: Annual Report 2020. [https://www.eurotransplant.org/wp-content/uploads/2021/08/ETP\\_AR2020\\_opm\\_LR.pdf](https://www.eurotransplant.org/wp-content/uploads/2021/08/ETP_AR2020_opm_LR.pdf) Accessed 2022-04-03
- Nemati, E., Einollahi, B., Pezeshki, M.L., Porfarziani, V., Fattahi, M.R.: Does Kidney Transplantation with Deceased or Living Donor Affect Graft Survival? *Nephro-Urology Monthly* **6**(4) (2014)
- Ellison, B.: A Systematic Review of Kidney Paired Donation: Applying Lessons From Historic and Contemporary Case Studies to Improve The US Model. *Wharton Research Scholars* **107** (2014)
- Biró, P., van de Klundert, J., Manlove, D., Pettersson, W., Andersson, T., Bunapp, L., Chromy, P., Delgado, P., Dworczak, P., Haase, B., Hemke, A., Johnson, R., Klimentova, X., Kuypers, D., Costa, A.N., Smeulders, B., Spieksma, F., Valentín, M.O., Viana, A.: Modelling and Optimisation in European Kidney Exchange Programmes. *European Journal of Operational Research* **291**(2), 447–456 (2021)
- Breuer, M., Meyer, U., Wetzel, S., Mühlfeld, A.: A Privacy-Preserving Protocol for the Kidney Exchange Problem. *WPES* (2020)
- Breuer, M., Meyer, U., Wetzel, S.: Privacy-Preserving Maximum Matching on General Graphs and its Application to Enable Privacy-Preserving Kidney Exchange. In: *ACM Conference on Data and Application Security and Privacy (CODASPY)* (2022)
- Pansart, L., Cambazard, H., Catusse, N., Stauffer, G.: Kidney Exchange Problem: Models and Algorithms. In: *HAL Archives-ouvertes* (2014)
- Carvalho, M., Klimentova, X., Glorie, K., Viana, A., Constantino, M.: Robust Models for the Kidney Exchange Problem. *Inform Journal on Computing* (2020)
- Ashby, V.B., Leichtman, A.B., Rees, M.A., Song, P.X.-K., Bray, M., Wang, W., Kalbfleisch, J.D.: A Kidney Graft Survival Calculator that Accounts for Mismatches in Age, Sex, HLA, and Body Size. *Clinical Journal of the American Society of Nephrology*, 1148–1160 (2017)
- Abraham, D.J., Blum, A., Sandholm, T.: Clearing Algorithms for Barter Exchange Markets: Enabling Nationwide Kidney Exchange. In: *ACM Conference on Electronic Commerce* (2007). ACM
- Fouque, P.-A., Poupard, G., Stern, J.: Sharing Decryption in the Context of Voting or Lotteries. In: *International Conference on Financial Cryptography*, pp. 90–104 (2000). Springer
- Shamir, A.: How to Share a Secret. *Communications of the ACM* **22**(11) (1979)
- Keller, M.: MP-SPDZ: A Versatile Framework for Multi-Party Computation. In: *CCS '20: 2020 ACM SIGSAC Conference on Computer and Communications Security* (2020)
- Pape, U., Conrad, D.: Maximales Matching in Graphen. In: *Ausgewählte Operations Research Software in FORTRAN* (1980)
- Sung, Y.C.: The HLA System: Genetics, Immunology, Clinical Testing, and Clinical Implications. *Yonsei medical journal* **48** (2007)
- Eurotransplant: Histocompatibility. In: *Eurotransplant Manual Ver. 4.5*, (2018). Chap. 10
- Lefaucheur, C., Loupy, A., Hill, G.S., Andrade, J., Nochy, D., Antoine, C., Gautreau, C., Charron, D., Glotz, D., Suberbielle-Boissel, C.: Preexisting Donor-Specific HLA Antibodies Predict Outcome in Kidney Transplantation. *Journal of the American Society of Nephrology* (2010)
- Ntokou, I.-S.A., Iniotaki, A.G., Kontou, E.N., Darema, M.N., Apostolaki, M.D., Kostakis, A.G., Boletis, J.N.: Long-Term Follow Up for Anti-HLA Donor Specific Antibodies Postrenal Transplantation: High Immunogenicity of HLA Class II Graft Molecules. *Transplant International* (2011)
- Santos, C., Costa, R., Malheiro, J., Pedrosa, S., Almeida, M., Martins, L.S., Dias, L., Tafulo, S., Henriques, A.C., Antonio, C.: Kidney Transplantation Across a Positive Crossmatch: A Single-Center Experience. In: *Transplantation Proceedings* (2014)
- Eurotransplant: Kidney. In: *Eurotransplant Manual Ver. 4.5*, (2018). Chap. 4
- Leeaphorn, N., Pena, J.R.A., Thamcharoen, N., Khankin, E.V., Pavlakis, M., Cardarelli, F.: HLA-DQ Mismatching and Kidney Transplant Outcomes. *Journal of the American Society of Nephrology* (2018)
- Opelz, G., Döhler, B.: Association of HLA Mismatch with Death with a Functioning Graft after Kidney Transplantation: A Collaborative Transplant Study Report. *American Journal of Transplantation* (2012)
- Opelz, G.: Impact of HLA Compatibility on Survival of Kidney Transplants from Unrelated Live Donors. *Transplantation* (1997)
- Lim, W.H., Chadban, S.J., Clayton, P., Budgeon, C.A., Murray, K., Campbell, S.B., Cohny, S., Russ, G.R., McDonald, S.P.: Human Leukocyte Antigen Mismatches Associated with Increased Risk of Rejection, Graft Failure, and Death Independent of Initial Immunosuppression in Renal Transplant Recipients. *Clinical Transplantation* (2012)
- Nguyen, M.C.: Evaluation of HLA Typing Data and Transplant Outcome in Pediatric Renal Transplantation. PhD thesis, Medizinische Universität Wien (2021). <https://repositorium.meduniwien.ac.at/obvumwhs/content/titleinfo/5894916/full.pdf>
- Blutspenden: Rund Ums Blut. <https://www.blutspenden.de/rund-ums-blut/blutgruppen/> Accessed 2022-04-03

30. de Weerd, A.E., Betjes, M.G.H.: ABO-Incompatible Kidney Transplant Outcomes: A Meta-Analysis. *Clinical Journal of the American Society of Nephrology* (2018)
31. Waiser, J., Schreiber, M., Budde, K., Fritsch, L., Böhrer, T., Hause, I., Neumayer, H.-H.: Age-matching in Renal Transplantation. *Nephrology Dialysis Transplantation* (2000)
32. Zhoua, J.-Y., Chenga, J., Huang, H.-F., Shen, Y., Jiang, Y., Chen, J.-H.: The Effect of Donor-Recipient Sex Mismatch on Short- and Long-term Graft Survival in Kidney Transplantation: A Systematic Review and Meta-Analysis. *Clinical Transplantation* (2013)
33. Miller, A.J., Kiberd, B.A., Alwayn, I.P., Odutayo, A., Tennankore, K.K.: Donor-Recipient Weight and Sex Mismatch and the Risk of Graft Loss in Renal Transplantation. *Clinical Journal of the American Society of Nephrology* (2017)
34. El-Agroudy, A.E., Hassan, N.A., Bakir, M.A., Foda, M.A., Shokeir, A.A.: Effect of Donor/Recipient Body Weight Mismatch on Recipient and Graft Outcome in Living-Donor Kidney Transplantation. *American Journal of Nephrology* (2003)
35. Cho, H., Wu, D.J., Berger, B.: Secure Genome-Wide Association Analysis using Multiparty Computation. *Nature biotechnology* **36**(6), 547–551 (2018)
36. Bonte, C., Makri, E., Ardehshirdavani, A., Simm, J., Moreau, Y., Vercauteren, F.: Towards Practical Privacy-Preserving Genome-Wide Association Study. *BMC bioinformatics* **19**(1), 1–12 (2018)
37. Tkachenko, O., Weinert, C., Schneider, T., Hamacher, K.: Large-Scale Privacy-Preserving Statistical Computations for Distributed Genome-Wide Association Studies. In: 13. ACM ASIA Conference on Computer and Communications Security (ASIACCS'18), pp. 221–235. ACM, Songdo, South Korea (2018). <https://crypto.de/papers/TWSH18.pdf>
38. Schneider, T., Tkachenko, O.: EPISODE: Efficient Privacy-Preserving Similar Sequence Queries on Outsourced Genomic Databases. In: Proceedings of the 2019 ACM Asia Conference on Computer and Communications Security, pp. 315–327 (2019)
39. Günther, D., Holz, M., Judkewitz, B., Möllering, H., Pinkas, B., Schneider, T.: PEM: Privacy-Preserving Epidemiological Modeling. *Cryptology ePrint Archive* (2020)
40. Barni, M., Failla, P., Kolesnikov, V., Lazeretti, R., Sadeghi, A.-R., Schneider, T.: Secure Evaluation of Private Linear Branching Programs with Medical Applications. In: 14. European Symposium on Research in Computer Security (ESORICS'09), pp. 424–439 (2009)
41. Barni, M., Failla, P., Lazeretti, R., Sadeghi, A.-R., Schneider, T.: Privacy-Preserving ECG Classification with Branching Programs and Neural Networks. *IEEE Transactions on Information Forensics and Security* (TIFS), 452–468 (2011)
42. Yao, A.C.-C.: How to Generate and Exchange Secrets. In: 27th Annual Symposium on Foundations of Computer Science (SFCS 1986) (1986)
43. Malkhi, D., Nisan, N., Pinkas, B., Sella, Y.: Fairplay — A Secure Two-Party Computation System. In: 13. USENIX Security Symposium (USENIX Security'04) (2004)
44. Kolesnikov, V., Schneider, T.: Improved Garbled Circuit: Free XOR Gates and Applications. In: Automata, Languages and Programming. *Lecture Notes in Computer Science* (2008)
45. Zahur, S., Rosulek, M., Evans, D.: Two Halves Make a Whole. In: Advances in Cryptology - EUROCRYPT 2015. *Lecture Notes in Computer Science* (2015)
46. Patra, A., Schneider, T., Suresh, A., Yalame, H.: ABY2.00: Improved Mixed-Protocol Secure Two-Party Computation. In: 30th USENIX Security Symposium (USENIX Security 21), pp. 2165–2182 (2021)
47. Järvinen, K., Leppäkoski, H., Lohan, E.-S., Richter, P., Schneider, T., Tkachenko, O., Yang, Z.: PILOT: Practical Privacy-Preserving Indoor Localization Using Outsourcing. In: IEEE European Symposium on Security and Privacy (EuroS&P) (2019)
48. Goldreich, O., Micali, S., Wigderson, A.: How to Play ANY Mental Game. In: Proceedings of the 19th Annual ACM Symposium on Theory of Computing. STOC '87 (1987)
49. Wiesner, S.: Conjugate coding. *ACM SIGACT News* **15**(1) (1983)
50. Rabin, M.O.: How to Exchange Secrets with Oblivious Transfer (1981)
51. Asharov, G., Lindell, Y., Schneider, T., Zohner, M.: More Efficient Oblivious Transfer Extensions. *Journal of Cryptology* **30**(3) (2017)
52. Ben-Or, M., Goldwasser, S., Wigderson, A.: Completeness Theorems for Non-Cryptographic Fault-Tolerant Distributed Computation. In: Proceedings of the Twentieth Annual ACM Symposium on Theory of Computing (1988)
53. Beaver, D.: Efficient Multiparty Protocols using Circuit Randomization. In: Annual International Cryptology Conference (1991)
54. Demmler, D., Schneider, T., Zohner, M.: ABY - A Framework for Efficient Mixed-Protocol Secure Two-Party Computation. *Network and Distributed System Security Symposium (NDSS)* (2015)
55. Rathee, D., Schneider, T., Shukla, K.: Improved Multiplication Triple Generation over Rings via RLWE-based AHE. In: International Conference on Cryptology and Network Security (2019)
56. Braun, L., Cammarota, R., Schneider, T.: POSTER: A Generic Hybrid 2PC Framework with Application to Private Inference of Unmodified Neural Networks (Extended Abstract). *Privacy in Machine Learning Workshop (PriML@NeurIPS'21)* (2021)
57. Kamara, S., Raykova, M.: Secure Outsourced Computation in a Multi-Tenant Cloud. In: IBM Workshop on Cryptography and Security in Clouds (2011)
58. Damgård, I., Pastro, V., Smart, N., Zakarias, S.: Multiparty Computation from Somewhat Homomorphic Encryption. In: Advances in Cryptology - CRYPTO 2012 (2012)
59. Biró, P., Cechlárová, K.: Inapproximability of the Kidney Exchange Problem. *Information Processing Letters* **101**(5), 199–202 (2007)
60. Desai, T., Ritchie, F., Welpton, R.: Five safes: designing data access for research. Technical report, University of the West of England (2016)
61. European Data Protection Board: Recommendations 01/2020 on measures that supplement transfer tools to ensure compliance with the EU level of protection of personal data (2021)
62. Araki, T., Furukawa, J., Ohara, K., Pinkas, B., Rosemarin, H., Tsuchida, H.: Secure Graph Analysis at Scale. In: Proceedings of the 2021 ACM SIGSAC Conference on Computer and Communications Security, pp. 610–629 (2021)
63. Naor, M., Pinkas, B., Pinkas, B.: Efficient Oblivious Transfer Protocols. In: Proceedings of the Twelfth Annual ACM-SIAM Symposium on Discrete Algorithms (2001)
64. Ishai, Y., Kilian, J., Nissim, K., Petrank, E.: Extending Oblivious Transfers Efficiently. In: Advances in Cryptology - CRYPTO 2003, vol. 2729 (2003)
65. Guo, C., Katz, J., Wang, X., Yu, Y.: Efficient and Secure Multiparty Computation from Fixed-Key Block Ciphers. In: 2020 IEEE Symposium on Security and Privacy (SP), pp. 825–841 (2020). IEEE

## Appendix

### Additional MPC Subprotocols

This part of the Appendix contains additional protocols of our MPC-based PPKE solution, SPIKE, that are similar to the ones presented in the main part and, thus, referred to the appendix.

### Additional Protocols for the Compatibility Matching

This subsection presents additional subprotocols for the compatibility matching phase.

---

## Subprotocol 7 $\text{evalHLA}(\langle \text{hla}_d \rangle^B: \text{vector}, \langle \text{hla}_r \rangle^B: \text{vector})$

---

→ int

```

1:  $\langle \text{mm} \rangle^B \leftarrow \{ \langle 0 \rangle^B \}^{|\text{HLA}|}$ 
2: for  $i = 0, \dots, |\text{HLA}| - 1$  do
3:    $\langle \text{mm} \rangle^B \leftarrow \langle \text{hla}_d \rangle^B[i] \oplus \langle \text{hla}_r \rangle^B$ 
4: end for
5:  $\langle \text{sum} \rangle^B \leftarrow \text{HammingW}(\{ \langle 0 \rangle^B \}^{|\text{HLA}|}, \langle \text{mm} \rangle^B)$ 
6:  $\langle c \rangle^B \leftarrow \langle \text{sum} \rangle^B < \langle 5 \rangle^B$ 
7:  $\langle b \rangle^B \leftarrow \langle \text{sum} \rangle^B < \langle 3 \rangle^B$ 
8:  $\langle a \rangle^B \leftarrow \langle \text{sum} \rangle^B == \langle 0 \rangle^B$ 
9: return  $\langle a \rangle^B ? \langle b \rangle^B : \langle c \rangle^B$ 

```

---

**HLA Antigen Comparison.** In Subprotocol 7, we compare the HLA antigens of the potential recipient and donor and determine the number of HLA mismatches. It takes two vectors  $\text{hla}_d$  and  $\text{hla}_r$ , with the HLA antigens

**Table 5** Encoding of the different blood groups.

Encoding	Blood Group
00	O
01	A
10	B
11	AB

of the donor and recipient respectively as input. The number of  $|HLA|$  is public as it is a fixed value. The vector  $mm$  indicates the HLA mismatches of the donor and the recipient. A mismatch occurs if either donor or recipient has a HLA antigen that the other does not have (cf. Line 3). For enhanced efficiency, we parallelize the comparison as SIMD operation such that the vector  $mm$  is computed in a single step. Afterwards, the number of HLA mismatches is determined with a Hamming Weight Circuit (cf. Line 5). Based on the number of mismatches, the subprotocol outputs an indicator for the quality of the pairing w.r.t. the HLA antigens: Class  $A$  is an optimal fit with no mismatches, class  $B$  is a good fit, and class  $C$  is an acceptable fit with 3-4 mismatches (cf. Lines 6-9). *MPC Cost.* Line 3 in Subprotocol 7 evaluates  $|HLA| \times XOR$  gates (as SIMD). Line 5 evaluates one Hamming Distance circuit. Lines 6-9 contain three comparison and three MUX gates. Thus, the circuit's multiplicative depth is 7, which is determined by the number of AND gates on the longest path. Naively, using Yao's Garbled Circuits ( $\mathcal{Y}$ ) seems to be most efficient. However, considering that Subprotocol 1 is done in  $\mathcal{B}$  sharing, the conversion cost outweigh the benefits of using  $\mathcal{Y}$  instead of  $\mathcal{B}$ , thus,  $\mathcal{B}$  is used here as well.

---

**Subprotocol 8**  $\text{evalABO}(\langle bg_d \rangle^{\mathcal{B}} : \text{vector}, \langle bg_r \rangle^{\mathcal{B}} : \text{vector}) \rightarrow \text{int}$ 


---

- 1:  $\langle a \rangle^{\mathcal{B}} \leftarrow \neg((\langle bg_r \rangle^{\mathcal{B}}[0] \oplus \langle bg_d \rangle^{\mathcal{B}}[0]) \vee (\langle bg_r \rangle^{\mathcal{B}}[1] \oplus \langle bg_d \rangle^{\mathcal{B}}[1]))$
  - 2:  $\langle b \rangle^{\mathcal{B}} \leftarrow ((\langle bg_r \rangle^{\mathcal{B}}[1] \wedge \neg \langle bg_d \rangle^{\mathcal{B}}[0]) \vee (\langle bg_r \rangle^{\mathcal{B}}[0] \wedge \neg \langle bg_d \rangle^{\mathcal{B}}[1]))$
  - 3:  $\langle v \rangle^{\mathcal{B}} \leftarrow \langle a \rangle^{\mathcal{B}} \vee \langle b \rangle^{\mathcal{B}}$
  - 4: **return**  $\langle v \rangle^{\mathcal{B}} ? \langle \text{best}_{\text{age}} \rangle^{\mathcal{B}} : \langle 0 \rangle^{\mathcal{B}}$
- 

**ABO blood group comparison.** Subprotocol 8 contains the privacy-preserving evaluation of the compatibility of ABO blood groups of a donor and a recipient. It takes two two-bit vectors as input:  $bg_d \in \{0, 1\}^2$  is the blood group of the donor and  $bg_r \in \{0, 1\}^2$  is the blood group of the recipient. The blood group encoding is shown in Table 5. Lines 1-2 ensure that the blood group of recipient and donor are compatible, i.e., they have to be either equal,  $bg_r[1] > bg_d[0]$ , or  $bg_r[0] > bg_d[1]$  (cf. Table 2). *MPC Cost.* Here, we evaluate 14 XOR gates and five AND gates in total per donor/recipient pair. As XOR gates can be locally evaluated, they are "for free". Therefore, the AND gates and circuit depth determine which MPC protocol is most efficient.  $\mathcal{B}$  is slightly more efficient than  $\mathcal{Y}$  since the circuit depth is smaller than the number of total AND gates.

---

**Subprotocol 9**  $\text{evalAge}(\langle a_d \rangle^{\mathcal{B}} : \text{int}, \langle a_r \rangle^{\mathcal{B}} : \text{int}) \rightarrow \text{int}$ 


---

- 1:  $\langle \text{eq} \rangle^{\mathcal{B}} \leftarrow \langle a_d \rangle^{\mathcal{B}} == \langle a_r \rangle^{\mathcal{B}}$
  - 2:  $\langle \text{yg} \rangle^{\mathcal{B}} \leftarrow \neg \langle a_d \rangle^{\mathcal{B}} \wedge \langle a_r \rangle^{\mathcal{B}}$
  - 3: **return**  $\langle \text{yg} \rangle^{\mathcal{B}} ? ((\langle \text{eq} \rangle^{\mathcal{B}} ? \langle A \rangle^{\mathcal{B}} : \langle B \rangle^{\mathcal{B}}) : ((\langle \text{eq} \rangle^{\mathcal{B}} ? \langle A \rangle^{\mathcal{B}} : \langle 0 \rangle^{\mathcal{B}}))$
- 

**Age Comparison.** Subprotocol 9 evaluates the compatibility of a donor and recipient based on their age group. It takes the age group of the donor  $\langle a_d \rangle^{\mathcal{B}}$  and the age group of the recipient  $\langle a_r \rangle^{\mathcal{B}}$  as input. Line 1 checks if they are in the same age group and Line 2 evaluates whether the donor is in a younger age group than the recipient. Afterwards, we compute the respective weight of this donor and recipient constellation. Similarly, as in Subprotocol 7, class  $A$  indicates an optimal match, class  $B$  a good match, and  $Eq$  denotes that recipient and donor are in the same age group. *MPC Cost.* Subprotocol 9 contains one comparison, one inversion, one AND gate, and three MUX gates. As Line 1 and Line 2 are independent, similarly

as the two MUX gates in Line 3, the circuit depth is 3. Thus, this subprotocol is slightly more efficient in  $\mathcal{B}$  than in  $\mathcal{Y}$ .

---

**Subprotocol 10**  $\text{evalSex}(\langle s_d \rangle^{\mathcal{B}} : \text{int}, \langle s_r \rangle^{\mathcal{B}} : \text{int}) \rightarrow \text{int}$ 


---

- 1:  $\langle \text{eq} \rangle^{\mathcal{B}} \leftarrow \langle s_d \rangle^{\mathcal{B}} == \langle s_r \rangle^{\mathcal{B}}$
  - 2:  $\langle \text{fdmr} \rangle^{\mathcal{B}} \leftarrow \langle s_d \rangle^{\mathcal{B}} \wedge \neg \langle s_r \rangle^{\mathcal{B}}$
  - 3: **return**  $\langle \text{fdmr} \rangle^{\mathcal{B}} ? ((\langle \text{eq} \rangle^{\mathcal{B}} ? \langle A \rangle^{\mathcal{B}} : \langle 0 \rangle^{\mathcal{B}}) : ((\langle \text{eq} \rangle^{\mathcal{B}} ? \langle A \rangle^{\mathcal{B}} : \langle B \rangle^{\mathcal{B}}))$
- 

**Sex Comparison.** Subprotocol 10 evaluates the compatibility of a donor and recipient based on their sex. It takes two secret shares  $\langle s_d \rangle^{\mathcal{B}}$  and  $\langle s_r \rangle^{\mathcal{B}}$  as input which represent the sex of the donor and recipient, respectively. In Line 1, the subprotocol determines if the pair shares the same sex. Line 2 checks whether the donor is female and the recipient male. As final step, the output weight of this donor and recipient constellation is computed, i.e., the optimal combination ("Class A") with equal sex receives the highest weight, while a female donor and a male recipient are assigned the lowest weight (0).

*MPC Cost.* Subprotocol 10 evaluates one comparison, one inversion, one AND, and three MUX gates. As Line 1 and Line 2 as well as two of the MUX gates in Line 3 are independent, we have a circuit depth of 3. Thus, Subprotocol 10 is slightly more efficient in  $\mathcal{B}$  than in  $\mathcal{Y}$ .

---

**Subprotocol 11**  $\text{evalWeight}(\langle w_d \rangle^{\mathcal{B}} : \text{int}, \langle w_r \rangle^{\mathcal{B}} : \text{int}) \rightarrow \text{int}$ 


---

- 1: **return**  $\langle w_d \rangle^{\mathcal{B}} < \langle w_r \rangle^{\mathcal{B}} ? \langle 0 \rangle^{\mathcal{B}} : \langle A \rangle^{\mathcal{B}}$
- 

**Weight Comparison.** Subprotocol 11 evaluates the compatibility of a donor and recipient based on their weight. It takes two secret shares as input:  $\langle w_d \rangle^{\mathcal{B}}$  and  $\langle w_r \rangle^{\mathcal{B}}$  which represent the weight of the donor and recipient, respectively. If the donor weighs less than the recipient, it returns a secret shared 0, otherwise, it indicates a good fit (i.e., class "A" w.r.t. criteria weight).

*MPC Cost.* We evaluate only one comparison gate. As the evaluation of a single comparison is more efficient in  $\mathcal{Y}$  than in  $\mathcal{B}$  [54],  $\mathcal{Y}$  would be more efficient. However, the conversion cost outweigh this benefit which is why  $\mathcal{B}$  is used for this subprotocol as in the previous comparison protocols.

#### Additional Protocols for the Cycle Computation

---

**Subprotocol 12**  $\text{removeWeights}(\langle \text{compG} \rangle^{\mathcal{B}} : \text{matrix}) \rightarrow \text{matrix}$ 


---

- 1:  $\langle uG \rangle^{\mathcal{A}} \leftarrow \text{matrix} \in \langle 0 \rangle^{\mathcal{A}|\text{pairs}}$
  - 2: **for**  $i = 0, \dots, |\text{pairs}| - 1$  **do**
  - 3:     **for**  $j = 0, \dots, |\text{pairs}| - 1$  **do**
  - 4:          $\langle uG \rangle^{\mathcal{A}}[i][j] \leftarrow \text{b2a}(\langle \text{compG} \rangle^{\mathcal{B}}[i][j] > \langle 0 \rangle^{\mathcal{B}} ? \langle 1 \rangle^{\mathcal{B}} : \langle 0 \rangle^{\mathcal{B}})$
  - 5:     **end for**
  - 6: **end for**
  - 7: **return**  $\langle uG \rangle^{\mathcal{A}}$
- 

**Weight Removal.** In Subprotocol 12, we compute the unweighted compatibility graph which is used for determining the number of cycles for the desired cycle length. It takes the weighted compatibility graph  $\text{compG}$  as input. The number of donor-recipient pairs  $|\text{pairs}|$  is public. In Line 4, we remove the edge weights: If it is greater than 0, it is set to 1, otherwise to 0. As preparation for later processing, a conversion to  $\mathcal{A}$  is done.

*MPC Cost.* Subprotocol 12 evaluates  $|\text{pairs}|^2$  comparisons, MUX gates, and conversions. The comparisons and MUX gates are independent, which results in a circuit depth of 2. Due to the total number of AND gates, which is  $2 \times |\text{pairs}|$ , this subprotocol is most efficient in  $\mathcal{B}$ .

**kNN Sort Protocol.** Our next MPC subprotocol shown in Subprotocol 13 is a  $k$ -nearest neighbor sort (a slightly adapted version of the protocol in [47]) that identifies the  $k$  most robust cycles (i.e., with the highest likelihood to result in successful transplantations).

---

**Subprotocol 13**  $\text{kNNSort}(\langle \text{cyclesSet} \rangle^{\mathcal{Y}} : \text{vector of tuples}, k: \text{int}) \rightarrow \text{vector of cycles}$ 


---

```

1:  $\langle \text{sortedW} \rangle^{\mathcal{Y}} \leftarrow \emptyset$ 
2:  $\langle \text{sortedC} \rangle^{\mathcal{Y}} \leftarrow \emptyset$ 
3: for  $i = 0, \dots, k$  do
4:    $\langle \text{sortedW} \rangle^{\mathcal{Y}}.append(\langle 0 \rangle^{\mathcal{Y}})$ 
5:    $\langle \text{vertices} \rangle^{\mathcal{Y}} \leftarrow \emptyset$ 
6:   for  $j = 0, \dots, cLen - 1$  do
7:      $\langle \text{vertices} \rangle^{\mathcal{Y}}.append(\langle \text{pairs} \rangle^{\mathcal{Y}})$ 
8:   end for
9:    $\langle \text{sortedC} \rangle^{\mathcal{Y}}.append(\langle \text{vertices} \rangle^{\mathcal{Y}})$ 
10: end for
11: for  $i = 0, \dots, |\text{cyclesSet}| - 1$  do
12:    $\langle \text{sortedW} \rangle^{\mathcal{Y}}[k] \leftarrow \langle \text{cyclesSet} \rangle^{\mathcal{Y}}[i][0]$ 
13:    $\langle \text{sortedC} \rangle^{\mathcal{Y}}[k] \leftarrow \langle \text{cyclesSet} \rangle^{\mathcal{Y}}[i][1]$ 
14:   for  $j = 0, \dots, k - 1$  do
15:      $\langle \text{sel} \rangle^{\mathcal{Y}} \leftarrow \langle \text{sortedW} \rangle^{\mathcal{Y}}[j] > \langle \text{sortedW} \rangle^{\mathcal{Y}}[j - 1]$ 
16:      $\langle \text{tmp1} \rangle^{\mathcal{Y}} \leftarrow \langle \text{sortedW} \rangle^{\mathcal{Y}}[j]$ 
17:      $\langle \text{tmp2} \rangle^{\mathcal{Y}} \leftarrow \langle \text{sortedW} \rangle^{\mathcal{Y}}[j - 1]$ 
18:      $\langle \text{sortedW} \rangle^{\mathcal{Y}}[j] \leftarrow \langle \text{sel} \rangle^{\mathcal{Y}} ? \langle \text{tmp2} \rangle^{\mathcal{Y}} : \langle \text{tmp1} \rangle^{\mathcal{Y}}$ 
19:      $\langle \text{sortedW} \rangle^{\mathcal{Y}}[j - 1] \leftarrow \langle \text{sel} \rangle^{\mathcal{Y}} ? \langle \text{tmp1} \rangle^{\mathcal{Y}} : \langle \text{tmp2} \rangle^{\mathcal{Y}}$ 
20:     for  $l = 0, \dots, cLen - 1$  do
21:        $\langle \text{tmp1} \rangle^{\mathcal{Y}} \leftarrow \langle \text{sortedC} \rangle^{\mathcal{Y}}[j][l]$ 
22:        $\langle \text{tmp2} \rangle^{\mathcal{Y}} \leftarrow \langle \text{sortedC} \rangle^{\mathcal{Y}}[j - 1][l]$ 
23:        $\langle \text{sortedC} \rangle^{\mathcal{Y}}[j][l] \leftarrow \langle \text{sel} \rangle^{\mathcal{Y}} ? \langle \text{tmp2} \rangle^{\mathcal{Y}} : \langle \text{tmp1} \rangle^{\mathcal{Y}}$ 
24:        $\langle \text{sortedC} \rangle^{\mathcal{Y}}[j - 1][l] \leftarrow \langle \text{sel} \rangle^{\mathcal{Y}} ? \langle \text{tmp1} \rangle^{\mathcal{Y}} : \langle \text{tmp2} \rangle^{\mathcal{Y}}$ 
25:     end for
26:   end for
27: end for
28:  $\langle \text{result} \rangle^{\mathcal{Y}} \leftarrow \emptyset$ 
29: for  $i = 0, \dots, |\text{cycles}| - 1$  do
30:    $\langle \text{result} \rangle^{\mathcal{Y}}.append(\text{tuple}(\langle \text{sortedW} \rangle^{\mathcal{Y}}[i], \langle \text{sortedC} \rangle^{\mathcal{Y}}[i]))$ 
31: end for
32: return  $\langle \text{result} \rangle^{\mathcal{Y}}$ 

```

---

It takes a secret shared vector of tuples  $\text{cyclesSet}$  with exchange cycles and their respective weights and  $k$  as input. The length of  $\text{cycles}$   $cLen$  is a public parameter. First, the subprotocol iterates over all cycles in  $|\text{cyclesSet}|$  to perform an insertion sort. Each cycle and the respective weight are added to  $\text{sortedC}$  and  $\text{sortedW}$  if its weight is one of the  $k$  highest weights (cf. Lines 11 to 27). Thus, the final  $\text{sortedW}$  and  $\text{sortedC}$  are sorted in decreasing order with respect to the weights of cycles.

*MPC Cost.* This subprotocol evaluates  $|\text{cyclesSet}| \times k$  comparisons and  $|\text{cyclesSet}| \times k \times (1 + cLen)$  MUX gates. It is most efficient in  $\mathcal{Y}$  due to depth of the circuit determined by the number of AND gates.

**Duplicate Removal.** Subprotocol 14 removes all duplicated exchange cycles and outputs the remaining  $|\text{unique}| = \lfloor \frac{|\text{cycles}|}{cLen} \rfloor$  cycles.

It takes a secret shared vector of tuples  $\text{sortedCycles}$  as input, which contains cycles and weights sorted according to the respective weights (i.e., the output by Subprotocol 13). The number of existing cycles  $|\text{cycles}|$ , the number of unique cycles  $|\text{unique}|$ , and the cycle length  $cLen$  are public parameters. For each cycle  $c1$  in  $\text{sortedCycles}$ , it is checked if it is equal to any other cycle  $c2$  (cf. Lines 6 to 13). If this is the case, its weight is set to 0 (cf. Line 15). To each equality, it is evaluated if the vertex of  $c1$  at index  $l$  and the vertex of  $c2$  at index  $(l + k) \bmod cLen$  are identical (cf. Line 9). With Subprotocol 13,  $\text{sortedCycles}$  is sorted and only the  $|\text{unique}|$  cycles with the highest weight are returned. The number of unique cycles is  $|\text{unique}| = \lfloor \frac{|\text{cycles}|}{cLen} \rfloor$ .

*MPC Cost.* Subprotocol 14 has  $|\text{cycles}| \times \sum_{i=0}^{|\text{cycles}|} (cLen \times (cLen - 1))$  comparisons and AND gates,  $|\text{cycles}| \times \sum_{i=0}^{|\text{cycles}|} (cLen - 1)$  OR gates,  $|\text{cycles}|$  MUX gates. Including Subprotocol 13, this results in  $|\text{cycles}| \times |\text{unique}|$  comparison and MUX gates, and an additional  $|\text{cycles}| \times |\text{unique}| \times (1 + cLen)$  MUX gates. This subprotocol is most efficient in  $\mathcal{Y}$  due to the depth of the circuit created by AND gates.

---

**Subprotocol 14**  $\text{removeDuplicates}(\langle \text{sortedCycles} \rangle^{\mathcal{Y}} : \text{vector of tuples}) \rightarrow \text{vector of cycles}$ 


---

```

1: for  $i = 0, \dots, |\text{cycles}| - 1$  do
2:    $\langle c1 \rangle^{\mathcal{Y}} \leftarrow \langle \text{sortedCycles} \rangle^{\mathcal{Y}}[i][1]$ 
3:    $\langle \text{combDup} \rangle^{\mathcal{Y}} \leftarrow \langle 0 \rangle^{\mathcal{Y}}$ 
4:   for  $j = 0 : i$  do
5:      $\langle c2 \rangle^{\mathcal{Y}} \leftarrow \langle \text{sortedCycles} \rangle^{\mathcal{Y}}[j][1]$ 
6:     for  $k = 1, \dots, cLen - 1$  do
7:        $\langle \text{duplicate} \rangle^{\mathcal{Y}} \leftarrow \langle 1 \rangle^{\mathcal{Y}}$ 
8:       for  $l = 0, \dots, cLen - 1$  do
9:          $\langle \text{same} \rangle^{\mathcal{Y}} \leftarrow$ 
10:           $\langle c1 \rangle^{\mathcal{Y}}[l] == \langle c2 \rangle^{\mathcal{Y}}[(l + k) \bmod cLen]$ 
11:          $\langle \text{duplicate} \rangle^{\mathcal{Y}} \leftarrow \langle \text{duplicate} \rangle^{\mathcal{Y}} \wedge \langle \text{same} \rangle^{\mathcal{Y}}$ 
12:       end for
13:        $\langle \text{combDup} \rangle^{\mathcal{Y}} \leftarrow \langle \text{combDup} \rangle^{\mathcal{Y}} \vee \langle \text{duplicate} \rangle^{\mathcal{Y}}$ 
14:     end for
15:      $\langle \text{sortedCycles} \rangle^{\mathcal{Y}}[i][0] \leftarrow$ 
16:       $\langle \text{isDuplicate} \rangle^{\mathcal{Y}} ? \langle 0 \rangle^{\mathcal{Y}} : \langle \text{sortedCycles} \rangle^{\mathcal{Y}}[i][0]$ 
17: end for
18: return  $\text{kNNSort}(\langle \text{sortedCycles} \rangle^{\mathcal{Y}}, |\text{unique}|)$ 

```

---



---

**Subprotocol 15**  $\#\text{TotalCycles}() \rightarrow \text{int}$ 


---

```

1:  $|\text{allCycles}| \leftarrow |\text{pairs}|$ 
2: for  $i = 1, \dots, cLen - 1$  do
3:    $|\text{allCycles}| \leftarrow |\text{allCycles}| \cdot (|\text{pairs}| - i)$ 
4: end for
5: return  $|\text{allCycles}|$ 

```

---

**Total Number of Cycles.** Subprotocol 15 computes the maximum number of cycles that can exist in the compatibility graph. Each vertex must appear at most once in a cycle which limits the number of possible cycles. As the numbers of pairs  $|\text{pairs}|$  and the cycle length  $cLen$  are public, computation can be done on plaintext.

---

**Subprotocol 16** disjointSet( $\langle \text{cycles} \rangle^{\mathcal{B}}$ : vector of tuples,  $\langle \text{cCycle} \rangle^{\mathcal{B}}$ : vector, *count*: int)  $\rightarrow$  Boolean

---

```

1:  $\langle \text{disJ} \rangle^{\mathcal{B}} \leftarrow \emptyset$ 
2: for  $i = 0, \dots, \text{count} - 1$  do
3:    $\langle c \rangle^{\mathcal{B}} \leftarrow \langle \text{cycles} \rangle^{\mathcal{B}}[i][1]$ 
4:   for  $j = 0, \dots, \text{cLen} - 1$  do
5:     for  $k = 0, \dots, \text{cLen} - 1$  do
6:        $\langle \text{tmp} \rangle^{\mathcal{B}} \leftarrow \langle c \rangle^{\mathcal{B}}[j] == \langle \text{cCycle} \rangle^{\mathcal{B}}[k]$ 
7:        $\langle \text{disJ} \rangle^{\mathcal{B}}.append(\langle \text{tmp} \rangle^{\mathcal{B}})$ 
8:     end for
9:   end for
10:   $\langle \text{disJ} \rangle^{\mathcal{B}} \leftarrow \text{ORTREE}(\langle \text{disJ} \rangle^{\mathcal{B}})$ 
11: end for
12: return  $\neg \langle \text{disJ} \rangle^{\mathcal{B}}[0]$ 

```

---

#### Additional Protocols for the Solution Evaluation

**Disjoint Cycles.** Subprotocol 16 computes whether a cycle *cCycle* does not join vertices with other cycles of a set of cycles *cycles*. It takes as input the set of secret shared cycles *cycles*, the secret shared cycle *cCycle*, and the number of cycles in *cycles* *count*. If another cycle shares a vertex with *cCycle*, *disJ* is set to 1 (cf. Line 10). In Line 12, we invert the result for further evaluation.

**MPC Cost.** In this subprotocol, we evaluate  $|\text{cycles}| \times \text{cLen}$  (cf. Line 6). In Line 10, we evaluate  $\log_2(\text{cLen})$  OR gates. At the end, we evaluate one XOR gate. As the number of total AND gates is greater than the depth of the circuit, this subprotocol is most efficient in  $\mathcal{B}$ .

---

**Subprotocol 17** findMaximumSet( $\langle \text{cyclesSets} \rangle^{\mathcal{Y}}$ : vector of tuples,  $\langle \text{cycleW} \rangle^{\mathcal{Y}}$ : vector)  $\rightarrow$  tuple

---

```

1:  $\langle \text{weights} \rangle^{\mathcal{Y}} \leftarrow \emptyset$ 
2:  $\langle \text{tmp} \rangle^{\mathcal{Y}} \leftarrow \emptyset$ 
3: for  $i = 0, 1$  do
4:    $\langle \text{weights} \rangle^{\mathcal{Y}}.append(\langle 0 \rangle^{\mathcal{Y}})$ 
5:    $\langle \text{sets} \rangle^{\mathcal{Y}} \leftarrow \emptyset$ 
6:   for  $j = 0, \dots, |\text{unique}| - 1$  do
7:      $\langle \text{vertices} \rangle^{\mathcal{Y}} \leftarrow \emptyset$ 
8:     for  $j = 0, \dots, \text{cLen} - 1$  do
9:        $\langle \text{vertices} \rangle^{\mathcal{Y}}.append(\langle |\text{pairs}| \rangle^{\mathcal{Y}})$ 
10:    end for
11:     $\langle \text{tmp} \rangle^{\mathcal{Y}}.append(\langle \text{vertices} \rangle^{\mathcal{Y}})$ 
12:  end for
13:   $\langle \text{sets} \rangle^{\mathcal{Y}}.append(\langle \text{tmp} \rangle^{\mathcal{Y}})$ 
14: end for
15: for  $i = 0, \dots, |\text{unique}| - 1$  do
16:   $\langle \text{weights} \rangle^{\mathcal{Y}}[1] \leftarrow \langle \text{cycleW} \rangle^{\mathcal{Y}}[i]$ 
17:   $\langle \text{sets} \rangle^{\mathcal{Y}}[1] \leftarrow \langle \text{cyclesSets} \rangle^{\mathcal{Y}}[i]$ 
18:   $\langle \text{sel} \rangle^{\mathcal{Y}} \leftarrow \langle \text{weights} \rangle^{\mathcal{Y}}[1] > \langle \text{weights} \rangle^{\mathcal{Y}}[0]$ 
19:   $\langle \text{tmp1} \rangle^{\mathcal{Y}} \leftarrow \langle \text{weights} \rangle^{\mathcal{Y}}[1]$ 
20:   $\langle \text{tmp2} \rangle^{\mathcal{Y}} \leftarrow \langle \text{weights} \rangle^{\mathcal{Y}}[0]$ 
21:   $\langle \text{weights} \rangle^{\mathcal{Y}}[1] \leftarrow \langle \text{sel} \rangle^{\mathcal{Y}} ? \langle \text{tmp2} \rangle^{\mathcal{Y}} : \langle \text{tmp1} \rangle^{\mathcal{Y}}$ 
22:   $\langle \text{weights} \rangle^{\mathcal{Y}}[0] \leftarrow \langle \text{sel} \rangle^{\mathcal{Y}} ? \langle \text{tmp1} \rangle^{\mathcal{Y}} : \langle \text{tmp2} \rangle^{\mathcal{Y}}$ 
23:  for  $j = 0, \dots, |\text{unique}| - 1$  do
24:     $\langle \text{tmp1} \rangle^{\mathcal{Y}} \leftarrow \langle \text{sets} \rangle^{\mathcal{Y}}[1][j]$ 
25:     $\langle \text{tmp2} \rangle^{\mathcal{Y}} \leftarrow \langle \text{sets} \rangle^{\mathcal{Y}}[0][j]$ 
26:     $\langle \text{sets} \rangle^{\mathcal{Y}}[1][j] \leftarrow \langle \text{sel} \rangle^{\mathcal{Y}} ? \langle \text{tmp2} \rangle^{\mathcal{Y}} : \langle \text{tmp1} \rangle^{\mathcal{Y}}$ 
27:     $\langle \text{sets} \rangle^{\mathcal{Y}}[0][j] \leftarrow \langle \text{sel} \rangle^{\mathcal{Y}} ? \langle \text{tmp1} \rangle^{\mathcal{Y}} : \langle \text{tmp2} \rangle^{\mathcal{Y}}$ 
28:  end for
29: end for
30: return  $(\langle \text{weights} \rangle^{\mathcal{Y}}[0], \langle \text{sets} \rangle^{\mathcal{Y}}[0])$ 

```

---

**Maximum Set.** Subprotocol 17 computes the set of cycles with the highest sum of weights, thus, the set of cycles with the highest probability for successful transplantations. Note that we do not compute the globally optimal solution but a local optimum.

The subprotocol takes a secret shared vector of tuples *cycles* and a secret shared vector *weights* as input. *cycles* contains all sets of disjoint cycles and

*weights* contains the respective weights of the each set. The number of pairs  $|\text{pairs}|$  and the number of unique cycles  $|\text{unique}|$  are public parameters. This subprotocol is a slight variation of Subprotocol 13 adapted to here used data structures. The parameter  $k$  is fixed to 1 since we look for the set with the highest weight.

**MPC Cost.** This protocols evaluates  $|\text{unique}|$  comparison and  $2|\text{unique}|^2 + 2|\text{unique}|$  MUX gates. Due to the large number of MUX gates in combination with the number of AND gates determining the depth of the circuit, it is most efficient in  $\mathcal{Y}$  sharing.

#### Communication Improvement with ABY2.0

Implementing SPIKE in ABY2.0 [46] can further decrease the communication cost. As the respective protocols were implemented only very recently in MOTION2NX [56], we use ABY [54] in our benchmarks to show practicality and additionally discuss the improvements that can be achieved with ABY2.0 in the following.

ABY2.0's improvements for secure multiplication with two inputs decreases the communication of the first and second part, the compatibility matching and the cycle computation. The improvements to conversions between different sharing types additionally benefit the first and the second part as these parts contain the most conversions between  $\mathcal{B}$  and  $\mathcal{A}$ . Further, the optimizations for matrix multiplications are beneficial for the second part. Concretely, the communication of Protocol 2 decreases from  $3 \times \ell^2 + 24 \times \ell + 2 \times \ell \times \kappa$  bits to  $23 \times \ell + \ell \times \kappa$  bits in every iteration of the inner loop (without considering the subprotocols). Similarly, Protocol 3's communication can be reduced from  $\ell \times (\frac{\ell}{2} + 2 \times \kappa + 4 \times |\text{pairs}|^3 + 1.5)$  bits to  $\ell \times (\kappa + 2 \times |\text{pairs}|^3 + 3)$  bits, where  $\ell$  is the bitlength and  $\kappa$  is the security parameter.

#### ABY Security Assumptions and Guarantees

The ABY MPC framework [54] provides mixed-abstraction building blocks for the creation of highly efficient hybrid-protocol MPC applications in a semi-honest adversary setting. Independent of the specific circuit design, a number of base-OTs are executed in the beginning to setup OT Extensions. The used base-OT primitive [63] guarantees security under the Computational Diffie-Hellman (CDH) hardness assumption. Being closely related to the discrete logarithm problem, this assumption is known to not be quantum resistant. The OT Extension [51, 64] primitive uses fixed-key AES modeled as a random permutation. While still considered secure in a semi-honest setting, theoretical attacks in the active security setting have been demonstrated [65]. Furthermore, ABY relies on the random oracle assumption, implemented by the SHA256 hash function. Similarly, Yao's Garbled Circuits [42] (denoted by  $\mathcal{Y}$  in our protocols) directly rely on the random permutation assumptions, while Arithmetic and Boolean Sharing [48] (denoted by  $\mathcal{A}/\mathcal{B}$  in our protocols) indirectly rely on those assumptions as a source of randomness. Those protocols can achieve information-theoretical security given a true correlated randomness source.

#### Detailed Benchmark Results

Tables 6 to 8 show the detailed benchmark results for the setup and online phase in all three described network settings (A: LAN + 10 Gb/s, B: LAN + 1 Gb/s, C: WAN) and a cycle length of  $L = 2$ . Tables 9 and 10 show the results for a cycle length of  $L = 3$ .

Table 11, finally, compares the benchmark results of both reduced medical compatibility factor set and the full set. This benchmark was performed in the two network settings A and C, as above.

**Table 6** Comparison of the communication costs and setup and online runtimes of SPIKE for the three networking configurations A: LAN + 10Gb/s, B: LAN + 1Gb/s, C: WAN, and for cycle length  $L = 2$ . This table contains the aggregated total costs and the individual costs of Phase 1 (Compatibility Matching).

Pairs	Comm. [MiB]		Setup Phase [s]			Online Phase [s]		
	Setup	Online	A	B	C	A	B	C
<i>Total</i>								
2	0.1	0	0.021	0.021	0.78	0.04	0.039	2.1
4	1.1	0.1	0.052	0.051	1.7	0.075	0.08	3.1
6	3.4	0.3	0.1	0.11	2.5	0.15	0.15	4.3
8	5.6	0.4	0.13	0.17	3	0.17	0.18	4.4
10	12.7	0.8	0.22	0.24	4	0.28	0.29	5.8
12	19.5	1	0.37	0.34	4.4	0.46	0.37	6.6
14	55.8	2.3	0.61	0.68	7.4	0.8	0.88	12
16	95.4	3.4	0.94	1.1	11	1.2	1.3	15
18	159	5.1	1.4	1.6	15	1.8	1.9	18
20	412.1	11.8	2.9	4.9	34	4.2	7.4	30
22	617.8	16.6	4.2	5.2	47	6.3	6.4	36
24	823.3	21.1	5.5	6.7	64	8.4	8.5	42
26	1,104.8	27	7.2	8.7	81	11	11	49
28	1,281.6	30.2	8.3	10	93	13	13	53
30	1,608.3	36.5	10	13	120	17	17	59
32	2,202.9	48.3	14	19	150	24	24	71
34	2,999.7	63.8	18	22	200	33	33	85
36	3,971.7	82.2	24	26	260	44	43	100
38	5,036.2	101.8	29	35	320	57	57	120
40	6,394	126.6	37	45	400	75	75	140
2	0	0	0.0071	0.0065	0.31	0.015	0.015	0.85
4	0.1	0	0.0093	0.0087	0.42	0.016	0.015	0.85
6	0.2	0	0.012	0.013	0.52	0.017	0.017	0.85
8	0.4	0	0.016	0.016	0.62	0.019	0.018	0.84
<i>Phase 1: Compatibility Matching</i>								
10	0.6	0	0.02	0.021	0.62	0.021	0.021	0.85
12	0.8	0	0.026	0.025	0.65	0.024	0.024	0.85
14	1.2	0	0.031	0.032	0.72	0.028	0.028	0.86
16	1.5	0	0.036	0.038	0.75	0.034	0.031	0.86
18	1.9	0	0.047	0.045	0.82	0.033	0.033	0.86
20	2.4	0	0.053	0.054	0.85	0.039	0.039	0.88
22	2.9	0.1	0.055	0.065	0.87	0.045	0.046	0.88
24	3.4	0.1	0.071	0.073	0.9	0.05	0.049	0.89
26	4	0.1	0.075	0.083	1	0.051	0.056	0.9
28	4.6	0.1	0.077	0.085	1	0.059	0.06	0.91
30	5.3	0.1	0.081	0.088	1.1	0.068	0.067	0.97
32	6.1	0.1	0.084	0.09	1.1	0.071	0.069	0.98
34	6.8	0.1	0.087	0.092	1.1	0.079	0.083	0.97
36	7.7	0.1	0.093	0.099	1.2	0.085	0.089	0.97
38	8.6	0.2	0.093	0.11	1.2	0.091	0.098	0.99
40	9.5	0.2	0.094	0.11	1.2	0.1	0.1	1

**Table 7** Comparison of the communication costs and setup and online runtimes of SPIKE for the three networking configurations A: LAN + 10Gb/s, B: LAN + 1Gb/s, C: WAN, and for cycle length  $L = 2$ . This table contains individual costs of Phase 2 and 3 (Cycle Computation and Evaluation).

Pairs	Comm. [MiB]		Setup Phase [s]			Online Phase [s]		
	Setup	Online	A	B	C	A	B	C
<i>Phase 2: Cycle Computation</i>								
2	0	0	0.0099	0.0099	0.43	0.013	0.012	0.75
4	0.2	0	0.013	0.013	0.54	0.014	0.014	0.76
6	0.4	0.1	0.02	0.02	0.83	0.017	0.018	0.76
8	0.9	0.1	0.028	0.031	1	0.021	0.021	0.85
10	1.7	0.2	0.043	0.047	1.2	0.024	0.027	0.77
12	2.8	0.3	0.06	0.059	1.3	0.033	0.031	0.79
14	4.3	0.4	0.082	0.087	1.6	0.034	0.04	0.8
16	6.2	0.5	0.1	0.12	1.8	0.047	0.048	0.82
18	8.6	0.7	0.12	0.12	1.8	0.048	0.054	0.84
20	11.6	0.8	0.13	0.14	2	0.063	0.061	0.87
22	15.3	1	0.13	0.17	2	0.075	0.072	0.9
24	19.6	1.2	0.15	0.19	2.9	0.078	0.083	1.1
26	24.6	1.5	0.17	0.23	3.2	0.088	0.1	1.3
28	30.5	1.7	0.19	0.27	5	0.1	0.11	2.4
30	37.2	2	0.22	0.3	4.8	0.11	0.12	2
32	44.8	2.3	0.24	0.35	5.7	0.12	0.14	2.2
34	53.4	2.6	0.27	0.42	6.5	0.13	0.15	2.3
36	63	3	0.3	0.48	7.1	0.13	0.16	2.3
38	73.7	3.4	0.34	0.55	7.9	0.14	0.17	2.3
40	85.6	3.8	0.38	0.63	8.8	0.16	0.18	2.4
2	0.1	0	0.0023	0.0027	0.022	0.0086	0.0082	0.3
4	0.7	0.1	0.019	0.02	0.29	0.026	0.03	0.35
6	2.2	0.1	0.054	0.061	0.56	0.068	0.07	0.47
8	3.8	0.2	0.066	0.1	0.74	0.089	0.096	0.48
<i>Phase 3: Cycle Evaluation</i>								
10	8.6	0.4	0.12	0.13	1.2	0.14	0.16	0.56
12	13.4	0.5	0.21	0.2	1.6	0.22	0.2	0.66
14	35	0.9	0.38	0.41	3.6	0.37	0.43	0.94
16	57.3	1.3	0.62	0.66	5.6	0.6	0.69	1.2
18	90.2	1.8	0.98	1	8.5	0.87	0.95	1.4
20	181.2	3.3	1.9	2.2	17	1.7	1.9	2.3
22	255.2	4.4	2.7	2.9	23	2.4	2.5	3
24	332.8	5.3	3.6	3.8	30	3.1	3.1	3.7
26	431.8	6.5	4.7	4.9	39	4	4	4.5
28	514.4	7.2	5.5	5.7	46	4.7	4.7	5.3
30	635.1	8.4	6.9	7.3	57	6	5.9	6.4
32	815.8	10.4	8.9	12	73	7.5	9.7	8
34	1,037.4	12.8	11	12	92	9.4	9.3	10
36	1,292.4	15.4	15	14	110	12	10	12
38	1,567.8	18	18	19	140	14	14	15
40	1,894.4	21.2	22	23	170	18	18	18

**Table 8** Comparison of the communication costs and setup and online runtimes of SPIKE for the three networking configurations A: LAN + 10 Gb/s, B: LAN + 1 Gb/s, C: WAN and for cycle length  $L = 2$ . This table contains individual costs of Phase 4 (Solution Evaluation).

Pairs	Comm. [MiB]		Setup Phase [s]			Online Phase [s]		
	Setup	Online	A	B	C	A	B	C
<i>Part 4: Solution Evaluation</i>								
2	0	0	0.002	0.0016	0.0071	0.0038	0.0037	0.22
4	0.2	0	0.01	0.01	0.42	0.02	0.021	1.2
6	0.5	0.1	0.019	0.019	0.63	0.044	0.045	2.2
8	0.5	0.1	0.018	0.019	0.62	0.045	0.045	2.2
10	1.8	0.2	0.043	0.041	0.96	0.088	0.088	3.6
12	2.4	0.2	0.078	0.055	0.84	0.18	0.11	4.3
14	15.4	0.9	0.12	0.15	1.5	0.37	0.39	9.4
16	30.4	1.6	0.18	0.26	2.5	0.55	0.55	12
18	58.2	2.6	0.27	0.44	4	0.8	0.84	15
20	216.9	7.6	0.84	2.5	14	2.4	5.4	26
22	344.5	11.2	1.3	2	21	3.8	3.9	31
24	467.5	14.5	1.7	2.7	30	5.2	5.3	36
26	644.4	19	2.3	3.5	38	7.2	7.4	42
28	732.1	21.1	2.5	3.9	41	8.3	8.4	44
30	930.7	26	3.2	4.8	53	11	11	50
32	1,336.2	35.5	4.5	5.7	73	16	14	60
34	1,902.1	48.2	6.4	9.2	100	23	23	72
36	2,608.7	63.7	8.7	12	140	32	32	86
38	3,386.1	80.2	11	16	180	43	43	100
40	4,404.4	101.4	15	21	230	57	57	120



**Table 9** Comparison of the communication costs and setup and online runtimes of SPIKE for the three networking configurations A: LAN + 10 Gb/s, B: LAN + 1 Gb/s, C: WAN and for cycle length  $L = 3$ . This table contains the aggregated total costs and the individual costs of Phases 1 and 2 (Compatibility Matching and Cycle Computation).

Pairs	Comm. [MiB]		Setup Phase [s]			Online Phase [s]		
	Setup	Online	A	B	C	A	B	C
<i>Total</i>								
3	0.5	0.1	0.029	0.028	0.97	0.054	0.056	2.2
5	4	0.3	0.096	0.11	2.2	0.13	0.15	2.9
7	19.7	0.7	0.26	0.27	4.1	0.3	0.34	4.3
9	52.6	1.5	0.63	0.66	7.3	0.63	0.73	5.3
11	182.5	3.3	2	2.1	19	1.9	2	9.4
13	1,215.8	16.3	12	13	110	12	12	34
15	2,084.4	22.8	21	23	180	19	20	45
17	5,428.5	58.1	52	56	440	54	54	93
18	9,537.2	107.6	88	95	740	100	100	150
3	0.1	0	0.0079	0.0075	0.32	0.015	0.015	0.85
5	0.1	0	0.011	0.01	0.42	0.016	0.016	0.85
7	0.3	0	0.014	0.014	0.52	0.018	0.018	0.85
9	0.5	0	0.019	0.018	0.61	0.019	0.02	0.85
11	0.7	0	0.023	0.024	0.64	0.023	0.023	0.86
13	1	0	0.029	0.029	0.72	0.025	0.024	0.86
15	1.3	0	0.034	0.036	0.74	0.029	0.029	0.86
<i>Phase 1: Compatibility Matching</i>								
17	1.7	0	0.041	0.043	0.77	0.035	0.034	0.87
18	1.9	0	0.042	0.049	0.82	0.035	0.034	0.87
3	0.1	0	0.013	0.012	0.54	0.014	0.013	0.76
5	0.4	0	0.018	0.019	0.83	0.016	0.016	0.76
7	1.1	0.1	0.029	0.031	1	0.019	0.019	0.77
9	2.2	0.2	0.052	0.053	1.3	0.024	0.023	0.77
11	3.8	0.3	0.072	0.079	1.5	0.026	0.029	0.78
13	6.2	0.4	0.1	0.11	2	0.032	0.034	0.84
15	9.3	0.5	0.1	0.13	1.8	0.036	0.04	0.81
17	13.4	0.7	0.12	0.15	2	0.049	0.049	0.86
18	15.8	0.8	0.13	0.16	2.2	0.047	0.054	0.91

**Table 10** Comparison of the communication costs and setup and online runtimes of SPIKE for the three networking configurations A: LAN + 10 Gb/s, B: LAN + 1 Gb/s, C: WAN and for cycle length  $L = 3$ . This table contains the individual costs of Phases 3 and 4 (Cycle and Solution Evaluation).

Pairs	Comm. [MiB]		Setup Phase [s]			Online Phase [s]		
	Setup	Online	A	B	C	A	B	C
<i>Phase 3: Cycle Evaluation</i>								
3	0.3	0	0.0061	0.0068	0.1	0.022	0.022	0.42
5	3.4	0.2	0.06	0.071	0.6	0.089	0.1	0.53
7	17.9	0.6	0.2	0.21	2	0.22	0.27	0.71
9	49.1	1.2	0.54	0.56	4.8	0.53	0.63	1.1
11	172.4	2.6	1.8	2	16	1.7	1.7	2.2
13	1,005.9	9.1	11	12	89	9.1	9.1	9.6
15	1,773.8	12.8	19	21	160	16	16	16
17	4,213.3	26.5	47	50	370	38	38	39
18	6,735.8	42	79	82	590	65	65	65
3	0	0	0.0024	0.0022	0.011	0.0038	0.0059	0.22
5	0.1	0	0.0083	0.0082	0.32	0.014	0.014	0.75
7	0.5	0.1	0.016	0.017	0.54	0.039	0.04	1.9
9	0.8	0.1	0.024	0.025	0.64	0.057	0.056	2.6
11	5.5	0.4	0.078	0.087	1	0.19	0.19	5.5
13	202.7	6.9	0.81	1.4	14	2.4	2.5	22
15	300	9.5	1.1	1.8	18	3.6	3.7	27
<i>Phase 4: Solution Evaluation</i>								
17	1,200.1	30.9	4.1	6	64	15	16	53
18	2,783.8	64.8	9.2	13	150	36	36	87

**Table 11** Comparison of the setup and online runtimes of SPIKE for the reduced medical factor compatibility matching and the full set in the two main networking configurations A: LAN + 10 Gb/s, C: WAN.

Pairs	Comm. [MiB]		Setup Phase [s]		Online Phase [s]	
	Setup	Online	A	C	A	C
<i>Reduced Medical Factor Set</i>						
2	0.1	0	0.0084	0.34	0.045	3
50	14.9	0.3	0.14	1.7	0.26	3.4
100	59.8	1.1	0.29	4.4	0.81	4.4
150	134.7	2.5	0.55	8.5	1.9	5.8
200	239.5	4.4	0.91	15	3.8	7.7
250	374.4	6.9	1.4	23	6.4	11
300	539.2	9.9	2	31	9.4	14
350	734	13.4	2.5	41	14	20
400	958.8	17.5	3.2	53	18	26
450	1,213.6	22.1	4.2	65	25	32
500	1,498.3	27.3	5.3	80	31	37
550	1,813.1	33	6.3	96	38	48
600	2,157.8	39.3	7.2	110	45	56
650	2,532.5	46.1	9	130	53	64
<i>Full Medical Factor Set</i>						
2	0.1	0	0.013	0.88	0.047	3.4
50	44	11.8	0.51	4.6	1	5.2
100	177.1	47.1	1.3	14	4.7	12
150	399.2	105.9	2.8	29	12	24
200	710.5	188.3	5.1	48	22	41
250	1,110.9	294.3	7.6	71	35	64
300	1,600.4	423.8	12	100	51	92
350	2,179.1	576.8	14	140	66	120
400	2,846.8	753.4	18	180	86	160
450	3,603.7	953.5	23	230	110	200
500	4,449.6	1,177.2	28	280	140	250
550	5,384.7	1,424.4	35	340	170	300
600	6,408.9	1,695.2	41	410	200	350
650	7,522.2	1,989.5	48	480	240	420